



PONTIFICIA UNIVERSIDAD CATÓLICA DE CHILE
ESCUELA DE INGENIERÍA

**EXPANSION PLANNING UNDER
LONG-TERM UNCERTAINTY FOR
HYDROTHERMAL SYSTEMS WITH
VOLATILE RESOURCES**

BENJAMÍN MALUENDA PHILIPPI

Thesis submitted to the Office of Research and Graduate Studies
in partial fulfillment of the requirements for the degree of
Master of Science in Engineering

Advisors:

MATÍAS NEGRETE PINCETIC

DANIEL OLIVARES QUERO

Santiago de Chile, May 2017

© MMXVII, BENJAMÍN MALUENDA PHILIPPI



PONTIFICIA UNIVERSIDAD CATÓLICA DE CHILE
ESCUELA DE INGENIERÍA

**EXPANSION PLANNING UNDER
LONG-TERM UNCERTAINTY FOR
HYDROTHERMAL SYSTEMS WITH
VOLATILE RESOURCES**

BENJAMÍN MALUENDA PHILIPPI

Members of the Committee:

MATÍAS NEGRETE PINCETIC

DANIEL OLIVARES QUERO

ÁLVARO LORCA GÁLVEZ

JUAN CARLOS ARANEDA TAPIA

MATÍAS HUBE GINESTAR

Thesis submitted to the Office of Research and Graduate Studies
in partial fulfillment of the requirements for the degree of
Master of Science in Engineering

Santiago de Chile, May 2017

© MMXVII, BENJAMÍN MALUENDA PHILIPPI

The thinker tries to determine and to represent the nature of the world through logic. He knows that reason and its tool, logic, are incomplete—the way an intelligent artist knows full well that his brushes or chisels will never be able to express perfectly the radiant nature of an angel or a saint. Still they both try, the thinker as well as the artist, each in his way. They cannot and may not do otherwise. Because when a man tries to realize himself through the gifts with which nature has endowed him, he does the best and only meaningful thing he can do.

—HERMANN HESSE,
Narcissus and Goldmund

ACKNOWLEDGEMENTS

I want to first and foremost thank my parents, Fernando and Alejandra, for giving me the best formal and informal education a young man could ask for. Their unbending support and counseling have allowed me to do the things I love and become the person I am today.

I thank professors Matías Negrete and Daniel Olivares for introducing me to the fascinating industry of power systems and showing me the nobility of research endeavors. Their guidance was fundamental in the course of my graduate studies and professional development. Many thanks to professor Álvaro Lorca for his valuable feedback on my ideas and writings. A cheerful shout-out to my lab mates at the Optimization, Control and Markets group, who made everyday's work into a joyful experience.

I am grateful for the opportunity of spending three months learning and working on this project as a visiting student researcher at the Renewable and Appropriate Energy Lab in the University of California, Berkeley. I extend my heartfelt gratitude to those who warmly welcomed me there; in special, to Josiah Johnston, for his patience and passion in sharing his skills and ideals with me.

Finally, I cannot thank Cecilia enough for her love and encouragement through all my endeavors, especially during this work. I am deeply grateful for all the years we have shared and for her support in closing this stage of my life.

My Masters studies were supported by the National Commission for Scientific and Technological Research (CONICYT-PCHA/MagísterNacional/2016-22161429). This research was also partially funded by the Complex Engineering Systems Institute, ISCI (ICM-FIC: P05-004-F, CONICYT: FB0816), CORFO (Project 13CEI2-21803), and CONICYT/FONDAP/15110019.

TABLE OF CONTENTS

ACKNOWLEDGEMENTS	iv
LIST OF FIGURES	vii
LIST OF TABLES	ix
ABSTRACT	x
RESUMEN	xi
1. INTRODUCTION	1
1.1. Context	1
1.2. Power System Expansion Planning	2
1.2.1. Expansion Planning Problem Definition	2
1.2.2. Centralized and Market Based Decision Making	5
1.3. State of the Art	7
1.3.1. Representation of Operations	7
1.3.2. Representation of Uncertainty	9
1.3.3. Hydrothermal Coordination	10
1.4. Contributions	15
2. MODEL FORMULATION AND SOLUTION METHOD	17
2.1. Scenario and Temporal Structure	17
2.2. Notation Under One Long-Term Scenario	18
2.2.1. Sets and Indices	18
2.2.2. Parameters Under One Long-Term Scenario	19
2.2.3. Variables Under One Long-Term Scenario	20
2.3. Optimization Problem Under One Long-Term Scenario	21
2.4. Extension to Multiple Long-Term Scenarios	25
2.5. Solution Method	27

3. IMPLEMENTATION AND COMPUTATIONAL EXPERIMENTS	30
3.1. Problem Data and Setup	30
3.2. One Long-Term Scenario Hydrothermal Model	32
3.2.1. Representative Operational Days and Inflow Scenarios	32
3.2.2. Case Study 1: Hourly Resolution Versus Load Blocks	34
3.2.3. Case Study 2: Effects of Inter-annual Storage	40
3.2.4. Case Study 3: Robustness of the Expansion Plan	42
4. CONCLUSIONS	48
5. FUTURE WORK	50
REFERENCES	51
APPENDICES	56
A. Input Data	57

LIST OF FIGURES

1.1	Optimization problem structure for Expansion Planning.	3
1.2	Load block discretization procedure.	7
1.3	Representative interval selection procedure.	9
1.4	Schematic approaches to uncertainty in expansion planning.	11
1.5	Current, future and total water cost functions.	12
1.6	Iterative process diagram for EP with SDDP.	13
2.1	One long-term scenario structure with inflow scenario trees in each investment period.	17
2.2	Long-term scenario tree structure with one nominal scenario and two extreme scenarios.	26
3.1	Schematic investment cost functions for transmission projects.	31
3.2	Schematic of water networks in the two most relevant hydraulic basins of Chile.	32
3.3	Hydrologies clustered into 3 groups, with representative year highlighted.	33
3.4	Inflow scenario structure for one long-term scenario.	34
3.5	Aggregated daily net load curves grouped in 4 clusters with representative date highlighted.	35
3.6	Generation investment plans yielded by the LB and RD models for 2.5 GW of must-build reservoir hydro new capacity.	36
3.7	Expected costs for the production costing simulations of the investment plans generated by the LB and RD models for the 2.5 GW new hydro case.	38

3.8	Comparison of expected dumped energy and unserved load in production costing simulations of the investment plans rendered by the RD and LB models.	39
3.9	Tree diagram of long-term nominal and extreme scenarios.	44
3.10	Total costs of the nominal long-term scenario under different cost caps for each extreme scenario.	46
3.11	Solver wall clock time under different cost caps for each extreme long-term scenario.	46
A.1	Total water inflows per registered annual hydrology in units of electric energy, with representative and extreme hydrologies highlighted.	60

LIST OF TABLES

3.1	Generator technologies with average characteristics.	31
3.2	Total Cost and Operational metrics of LB and RD investment plans	40
3.3	Total investment costs (Billion 2015US\$)	41
3.4	Average wall clock time per process (s).	41
3.5	Total cost bounds (Billion 2015 US\$) for each extreme long-term scenario. . .	45
A.1	Generation technologies.	57
A.2	Generators.	57
A.3	Fuel costs per period.	60
A.4	Transmission lines.	61
A.5	Transmission line parameters.	61

ABSTRACT

The significant integration of volatile renewable energy sources in power systems has raised concerns that motivate the use of greater operational details in expansion planning. Economic and reliable investment plans in this new paradigm can be obtained through the development of improved tools for electricity generation and transmission infrastructure planning. In this regard, this work proposes a stochastic programming model for planning the expansion of hydrothermal power systems. The model considers representative days with high temporal resolution and uncertainty in water inflows. This allows to capture inter-hourly phenomena such as load and renewable profile chronologies, ramping constraints and energy storage management. In addition, multiple long-term scenarios in the investment scale are included to obtain investment plans that yield reliable operations under extreme conditions. The Progressive Hedging Algorithm is applied to decompose the problem on a long-term scenario basis and to use computational resources efficiently. Numerical experiments on the Chilean power system show that the use of representative days outperforms the use of load blocks in both cost and reliability metrics. Results also show that reservoir hydroelectric plants provide higher flexibility to the system, enabling an economic and reliable integration of volatile and intermittent resources. Experiments also illustrate the impacts of considering extreme long-term scenarios in the obtained investment plans.

Keywords: Hydrothermal power systems, power system expansion planning, progressive hedging algorithm, stochastic programming, long-term uncertainty.

RESUMEN

La significativa integración de fuentes renovables volátiles de energía en los sistemas de potencia da pie a preocupaciones que motivan el uso de mayores detalles operacionales en la planificación de expansión de capacidad. Planes de inversión más económicos y confiables pueden ser obtenidos en este nuevo paradigma a través del desarrollo de mejores herramientas de planificación para infraestructura de generación y transmisión eléctrica. En este contexto, este trabajo presenta un modelo de programación estocástica para planificar la expansión de sistemas de potencia hidrotérmicos. El modelo considera incertidumbre en los afluentes de agua y días representativos con alta resolución temporal. Esto permite capturar fenómenos inter-horarios, como cronología de perfiles de demanda y recursos renovables, restricciones de rampa y manejo de embalses. En adición, se incluyen escenarios de largo plazo para obtener planes de inversión confiables bajo condiciones extremas. El algoritmo Progressive Hedging es aplicado para descomponer el problema de optimización en sus escenarios de largo plazo y usar los recursos computacionales de manera eficiente. Experimentos numéricos sobre el sistema eléctrico de Chile muestran que el uso de días representativos supera al uso de bloques de demanda en métricas de costo y confiabilidad. Los resultados también muestran que las plantas hidroeléctricas de embalse proveen mayor flexibilidad al sistema, permitiendo una integración económica y confiable de recursos volátiles. Los experimentos también ilustran el impacto de considerar escenarios de largo plazo sobre los planes de inversión obtenidos.

Palabras Claves: Generación eléctrica hidrotérmica, planificación de sistemas de potencia, algoritmo progressive hedging, programación estocástica, incertidumbre de largo plazo.

1. INTRODUCTION

1.1. Context

The impending threat of a climate change caused by anthropogenic greenhouse-gas emissions has moved nations to adopt transformative actions. The Paris Agreement reached in 2015 includes significant emissions reduction pledges related to the energy sector, which require that unprecedented amounts of renewable energy sources be incorporated into power grids. This raises several challenges, since according to the International Energy Agency (2016), “*structural changes to the design and operation of the power system are needed to ensure adequate incentives for investment and to integrate high shares of variable wind and solar power*”.

The power system industry is characterized by high capital cost investments on infrastructure and long project lifetimes. Hence, generation and transmission construction decisions have a strong impact on future operations. Plans for power system expansion and transformation must be elaborated rigorously in order to make it *flexible* and *robust* enough to assimilate variable and uncertain energy sources and be able to meet the projected load in a reliable manner.

Power system expansion planning models play a key role in easing the transition to low carbon grids and economies. The use of these models provides valuable insights to decision makers regarding system behavior and evolution, and allows estimating the impact of technologies, policies and external phenomena on the grid. Nevertheless, system interactions are becoming increasingly more complex, so these models must be adapted to a new paradigm by re-thinking some often used assumptions and simplifications.

1.2. Power System Expansion Planning

Transmission Expansion Planning (TEP) and Generation Expansion Planning (GEP) are tools that support investment decision making in the power system so that future electric demand may be satisfied in the most economic way with a desired level of reliability. These tools have been formalized into models through mathematical programming for more than half a century (Massé & Gibrat, 1957). GEP and TEP have traditionally been addressed separately, as computational power and optimization methods have not been able to cope with the size of coordinated problems up until recently. This work will refer indistinctly to either generation and/or transmission Expansion Planning as EP, given that problem structures are similar and decisions involved are analogous.

1.2.1. Expansion Planning Problem Definition

EP is formulated as an optimization problem whose objective is to minimize investment and operations costs over a certain time horizon. Size and timing of generation and/or transmission projects construction are key decision variables. Generator dispatch levels and power flow through transmission lines are variables that allow estimating the cost of operating the infrastructure decided by the model. This problem structure is termed a *bi-level program*, since the decisions taken at operations depend on the variable values of the investment level. The problem structure can be observed in the diagram in Figure 1.1.

The optimization problem presented in Figure 1.1 can be represented by a bi-level program written in the following compact manner for a multi-period horizon:

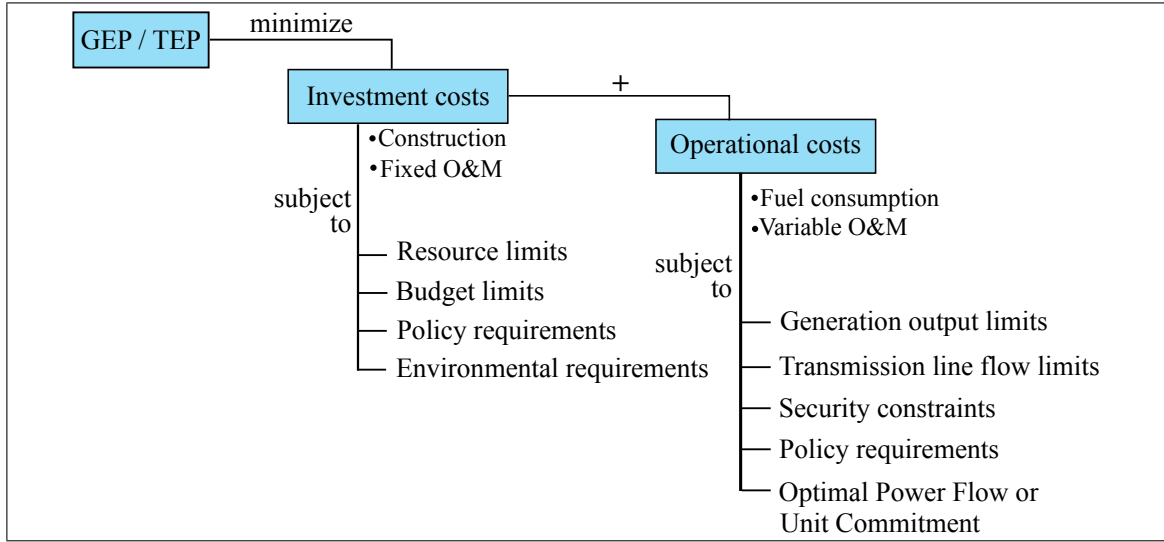


Figure 1.1. Optimization problem structure for Expansion Planning.

$$\min_{\mathbf{x}} \sum_{p \in \mathcal{P}} [c_p^\top \mathbf{x}_p + Q(p, \mathbf{x}_p)] \quad (1.1a)$$

$$\text{s.t.} \quad D \mathbf{x} \geq e \quad (1.1b)$$

$$\text{where } Q(p, \mathbf{x}_p) = \min_{\mathbf{y}_p} d_p^\top \mathbf{y}_p \quad (1.2a)$$

$$\text{s.t.} \quad W \mathbf{y}_p \geq u_p - T \mathbf{x}_p \quad (1.2b)$$

$$Z \mathbf{y}_p \geq v_p \quad (1.2c)$$

The objective function presented in (1.1a) minimizes total costs, which are the summation of both investment and operational costs over all studied periods. Investment decisions in each period represented by \mathbf{x}_p —size, location and type of generator units and transmission lines—are constrained by the equations in (1.1b), which describe the high-level problem. Such constraints include resource and budget bounds, as well as policy and environmental requirements. The latter have been included in the planning process only since recent decades, when the impacts of large electrical projects both on the natural

and social environments have began to be understood and considered relevant to decision-making.

Operational costs in each period are obtained through the low-level optimization program, where investments are taken as fixed variables and operational decisions represented by y_p —unit dispatch levels, line flows, storage management— are taken to minimize the cost of supplying load, summed in (1.2a). Constraints in (1.2b) link investment and operational variables together, by limiting dispatches and flows according to available capacity. Constraints in (1.2c) assure that operations are carried out in an economic and reliable manner. This may include constraining:

- Generation output levels
 - According to an economic dispatch, where units are allowed to freely adjust their output between timepoints.
 - Through a Unit Commitment formulation, where minimum up and down times, ramping limits and minimum generation levels must be obeyed.
- Transmission line flows
 - By a transport model, where it is assumed that line flows may be controlled, and voltage and angles are ignored. This is equivalent to any logistics model.
 - Using a Direct Current formulation, where angles can be taken into account.
 - With an Alternate Current model, where all the electric phenomena are considered.

Some models consider only continuous variables and compile optimization problems that are known as Linear Programs, which can be efficiently solved by commercial solvers. Other works propose models with binary and/or integer variables and are known as Mixed-Integer Linear Programs, which are harder to solve. These variables allow representing either discrete unit commitment in operations or discrete unit size construction. Moreover, some works present Non-Linear Programs to include generator heat rate curves, but have

to overlook details in other features to avoid unreasonable computation times. Commercial models and academic work take multiple assumptions and formulate different types of optimization programs. Whereas the structure may be the same, or similar, as the one exposed in (1.1a)–(1.2c), the specific variables, parameters and constraints may vary according to the study that is being carried out, in order to focus on key aspects and be able to model the studied system in a reasonable way.

Recent research on EP models has focused on:

- **Capturing greater operational detail** to better assess the costs of supplying demand once the investments have been carried out and obtain more flexible investment plans. Conventional controlled generation mixes have been assumed to be able to adjust their outputs to match smooth demand profiles without significant costs, but increasing shares of energy sources that can vary their outputs rapidly and uncontrollably are being incorporated in power grids.
- **Considering uncertainty endogenously** to obtain investment plans that hedge against multiple scenarios on an optimal way. Decision makers have traditionally run several deterministic case studies to get insights on each distinct scenario and then elaborated plans based on expert opinions or heuristic methods¹.
- **Modeling new technologies** to analyze their impact on system operations and evolution. Novel products and services that participate in the grid, such as electric vehicles, demand response, distributed generators, batteries, and others, offer distinct capabilities and may be added to conventional technologies.
- **Applying decomposition techniques** to reduce the computational time needed to reach a certain optimality gap. Decomposition methods allow harnessing the power of parallel and distributed computation, as well as reducing memory requirements in several cases.

¹The Merriam-Webster dictionary defines *heuristic* as an adjective that indicates “*involving or serving as an aid to learning, discovery, or problem-solving by **experimental** and especially **trial-and-error** methods*”

1.2.2. Centralized and Market Based Decision Making

Even though the problem definition presented in Section 1.2.1 is general and can accommodate any specific EP model, there has traditionally been a distinction in literature for different ways of representing decision making. Models were initially developed to aid central planners in vertically integrated power grids. Their goal was to minimize the social cost of expanding the grid and had the absolute attributions for executing any generation and transmission projects as needed. In recent decades, there has been an introduction of competition elements in several power grids around the globe, specially in the generation segment. In consequence, decisions on project construction are no longer made by a single agent, but by several firms that participate in markets.

Abundant academic literature has been published that aims to accommodate this new decision making paradigm and propose various EP models that take into account market considerations and competition, as the survey by Kagiannas et al. (2004) shows. Recent work has been done on simultaneous coordination of the GEP and TEP problems in thermal systems considering both single agent (Barati et al., 2015; Alizadeh & Jadid, 2011) and competitive environments (Pozo et al., 2013; Motamedi et al., 2010), such as Cournot competition. Consideration of both transmission and generation projects in the same planning process provides valuable insights to decision makers, even for a firm that participates in a single segment.

Despite the introduction of market elements in power system expansion, tools that render centralized expansion plans are still widely used by different parties:

Power System Companies: Centralized plans are a proxy for system expansion under perfect competition, so they can be used to estimate lower bounds for the returns of private investments.

Technology Developers: The value proposition of products and projects may be quantified by evaluating against a perfect competition proxy.

State and Regulatory Agencies: Even if decisions are not taken on a centralized manner, expansion models allow understanding system dynamics and interactions, as well as giving insights on the impact of economic and environmental policies.

Given its current validity and valuable applications, this work considers a centralized decision making approach, where expansion plans are formulated by minimizing social cost over the studied horizon.

1.3. State of the Art

1.3.1. Representation of Operations

An assumption that has been widely applied in EP models is that system load varies in a relatively slow manner, so that the only relevant operational costs and constraints are those of producing energy. This allows representing load through discrete *load blocks* instead of a chronological load profile. These blocks can be obtained by arranging the hourly demand curve of a specific time horizon on a decreasing order in what is called a *load duration curve*—typically one for each month—, and then discretized into a relatively small set of load blocks (Seifi & Sepasian, 2011). A scheme of this procedure can be observed in Fig. 1.2.

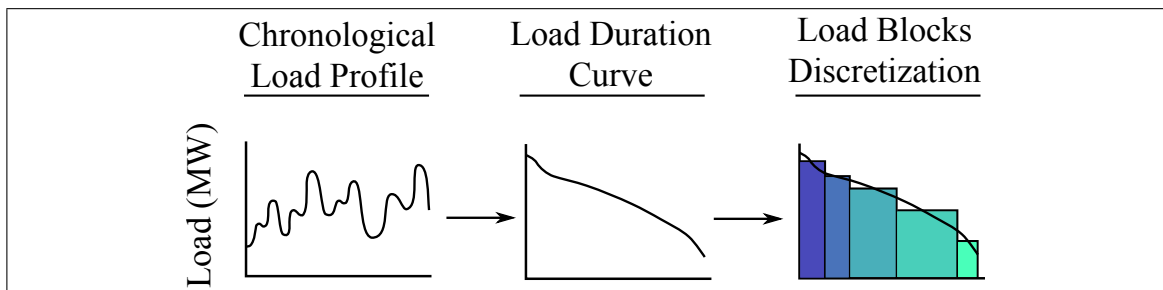


Figure 1.2. Load block discretization procedure.

The use of load blocks significantly reduces the size of the problem. A typical model may use between 5 and 10 blocks per month to represent load, which is a couple of orders

of magnitude less than the 720 or 744 hours encompassed in that interval. This simplification has been reasonably applied to conventional systems, where thermal and hydraulic generators are able to follow the smooth load profiles without significant costs additional to the production of energy.

Nevertheless, a larger share of renewable energy implies steep uncontrolled generation ramps. In the presence of these energy sources, conventional generators may not be able to provide enough flexibility in order to follow a no longer smooth net load curve. Alternatively, operational and maintenance costs could increase due to unit cycling, increased number of startups, and frequency variations. The load block procedure cannot model these inter-hour effects, such as ramping constraints or unit commitments. In addition, it fails to capture the chronology of load and renewable resource profiles. Thus, an investment plan produced by a model that considers a discrete representation of load may yield uneconomical or unreliable operations over its actual dispatch.

Several recent works have focused on better representing chronological operations' phenomena in the planning process. A novel approach proposed by Wogrin et al. (2016) consists on discretization of time-dependent parameters into *system states* rather than load blocks. This allows considering the temporal relation between load and renewable resource profiles when discretizing time into states. In addition, constraints between system states are formulated so that some chronology of the hours that they bundle is maintained. In the referenced paper, the authors manage to represent storage management in EP.

Another novel approach is the use of representative intervals with hourly resolution. These intervals may consist on days or weeks that are sampled from the studied horizon using different techniques and their hourly resolution allows modeling detailed operational constraints and concurrence of load and renewable resource profiles. Outputs of interest, such as costs and supplied energy, have to be scaled by the number of days or weeks that a certain selection represents. Nelson et al. (2012) applied this approach to study a large scale system with high resolution. This has also been applied by Palmintier & Webster (2016) to successfully incorporate a full Unit Commitment formulation into an EP model.

New technologies, such as demand response, have also been endogenously incorporated in EP models through this technique (Jonghe et al., 2012). Moreover, recent work by van Stiphout et al. (2017) has shown that considering highly detailed operational reserves can have significant impacts on the optimal investment plan. Fig. 3.5 exhibits a schematic for the sampling and modeling of representative intervals.

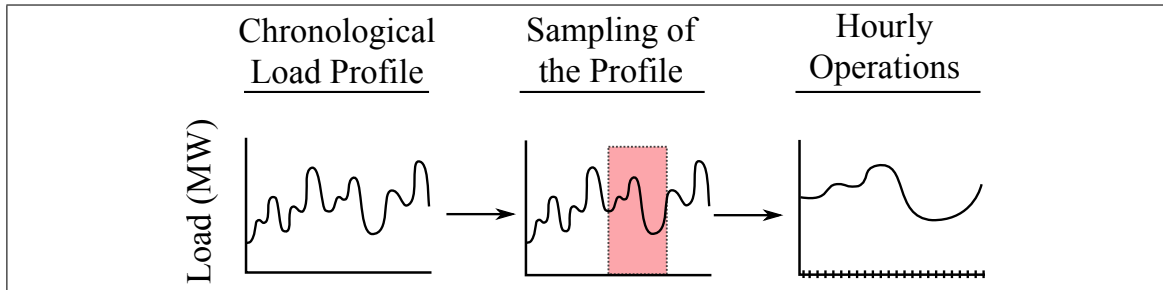


Figure 1.3. Representative interval selection procedure.

1.3.2. Representation of Uncertainty

One common simplification in early EP models was to take a deterministic approach, where a single scenario is taken into account in the optimization problem. The decision making process for an entity then involved running several individual case studies and deciding between the possible investment plans through expert knowledge or heuristic methods, such as minimizing the maximum regret or other rules (Velasquez et al., 2016).

Nonetheless, the increased volatility of energy resources' availability and cost has led to endogenously include uncertainty in EP. Thus, obtained investment plans are optimal considering several scenarios. Stochastic programming has been widely adopted to this extent². When the probability distribution of an uncertain phenomenon can be known or estimated through studies, then it is possible to discretize the distribution into a finite number of scenarios. Each scenario is then assigned a probability and the optimization minimizes total expected costs. This method has been applied in EP to account

²For outstanding educational material regarding Stochastic Programming and its application in several fields, please refer to Birge & Louveaux (1997).

for uncertain phenomena in the operational scale, such as daily wind profiles (Jin et al., 2014) and monthly load profiles (Park & Baldick, 2015). Stochastic programming leads not only to economic plans under uncertainty, but also to more reliable systems that can accommodate volatility

The use of discrete scenarios to represent parameter uncertainty has also been extended to the investment scale. A statistical extrapolation procedure to generate scenarios for load growth and fuel prices is presented and tested in an EP model by Feng & Ryan (2013). In contrast, Li et al. (2016) formulate discrete climate change effects scenarios according to expert opinions for EP. Even though there are works that use complex mathematical procedures to formulate discrete scenarios in the long term, there are doubts about whether it is methodologically correct to make decisions based on speculations that ignore singular events that may perturb long term trends or on opinions that may be slanted by imperfect knowledge or personal biases.

Robust Optimization (RO) is another tool that has been used to obtain reliable expansion plans when the probability distribution underlying an uncertain phenomenon is unknown. This approach considers that some parameters are uncertain and that their values will fall into distribution-free bounded intervals. The methodology then focuses on obtaining an optimal solution for the worst-case scenario under a certain defined degree of conservatism. Investment plans obtained this way are then hedged against the risk of those parameters taking the worst-case values. This methodology has been applied both to GEP (Dehghan et al., 2014) and to TEP (Dehghan et al., 2016).

Fig. 1.4 shows scenario tree diagrams that represent the three approaches described in this section.

1.3.3. Hydrothermal Coordination

Water reservoirs can be used in hydrothermal systems to hedge against different uncertainties and to provide flexibility in operations, since hydroelectric generators have fast

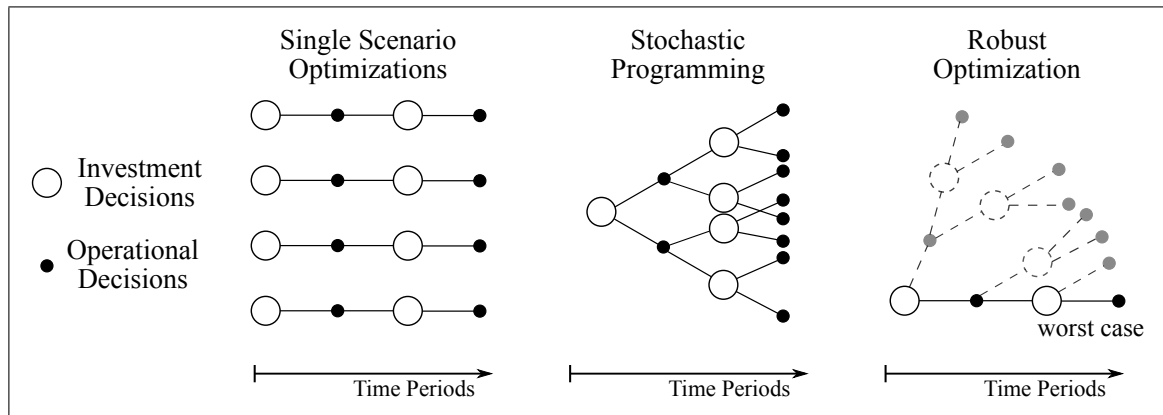


Figure 1.4. Schematic approaches to uncertainty in expansion planning.

ramp rates, no minimum up or down times, and no startup costs. Significant research has focused on modeling hydrothermal operations and including uncertainty of inflows themselves on the medium term—from weeks to months—, which is termed *hydrothermal coordination*. This problem has three characteristics which make it more difficult to address than purely thermal operations:

- (i) The use of stored water carries no immediate marginal cost that can be compared to that of thermal generators (i.e. fuel cost to produce an additional unit of energy) in order to determine optimal dispatches.
- (ii) Operational decisions are tightly linked between time points, since reservoir water levels depend on decisions taken in previous days and hours.
- (iii) The primary source of energy is inherently uncertain.

Even if the use of water to generate an additional unit of energy implies no marginal cost, it does have an opportunity cost. Water that is used in the present cannot be used in the future to displace expensive fuel-based generation. On the other hand, it may happen that the best time to use that water is actually the present. Fig. 1.5 shows how saving water for future times reduces the cost of power generation then, but increases the present generation cost, and vice-versa. System operators that control reservoir hydro power plants must solve this hydrothermal coordination problem to obtain optimal water values that

minimize the total cost of generation over the studied horizon. This value is then considered as a marginal cost in short term —days to weeks— operations planning. In power systems with wholesale markets, private owners of hydroelectric generator plants must solve a similar problem, but with the objective of finding an optimal bidding price that maximizes their return.

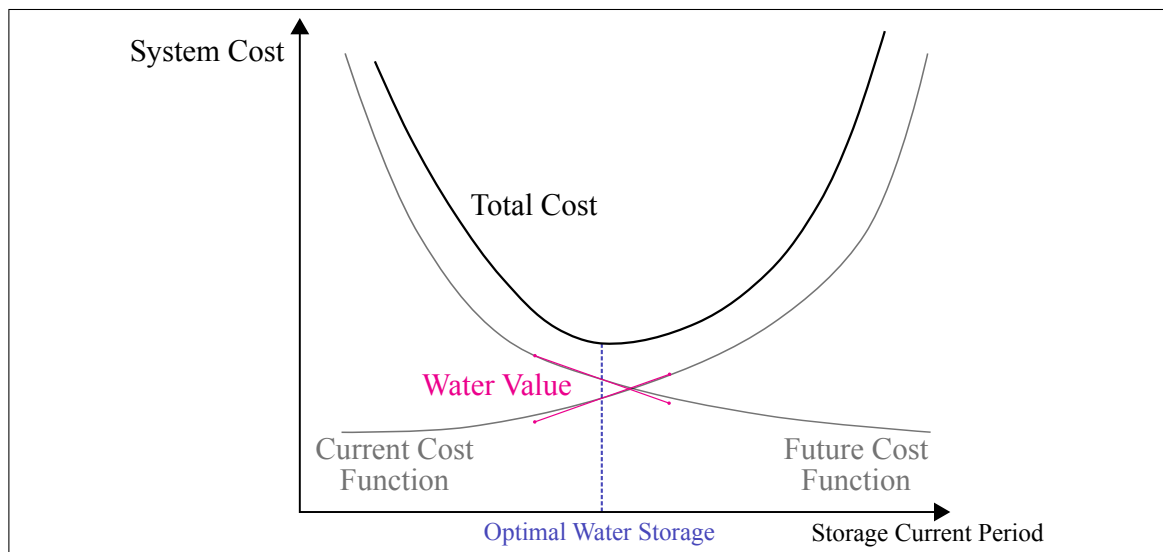


Figure 1.5. Current, future and total water cost functions.

Most hydrothermal Independent System Operators use the Stochastic Dual Dynamic Programming (SDDP) methodology first presented by Pereira & Pinto (1991) to consider large inflow scenario trees when coordinating operations. Derived formulations, such as the one by Abgottspon & Andersson (2016), allow solving the problem of the private company bidding in a wholesale market with the same methodology. SDDP offers the advantage of being able to solve multi-stage and multi-reservoir problems in reasonable computation times. Models based in this technique deliver operational policies that firms and operators can follow and assigns value to the use of water in each period, allowing the application of economic dispatches and unit commitments.

However, a recent review by Hemmati et al. (2013) finds that not enough attention has been paid on how to incorporate these operational procedures in EP models. Reservoir

management under various scenarios is a complex problem due to constraints that link the system state —reservoir water levels— throughout a time horizon. The SDDP methodology can successfully solve the hydrothermal coordination problem, but its optimal solution depends on the topology of the grid. Therefore, it cannot be endogenously incorporated in EP models to represent operations.

Some studies do use SDDP in EP through an iterative process (Campodónico et al., 2003; Oliveira et al., 2007; Vinasco et al., 2014). This is presented in Fig. 1.6. The EP problem is solved considering a simple representation of operations to obtain an investment plan. This is then passed on to a separate hydrothermal coordination model which is solved for the fixed proposed expansion plan with a large inflow scenario tree to obtain optimal water use strategies. Costs and decisions are contrasted with a convergence criterion (e.g. total costs change less than a certain percentage on successive iterations). If the criterion is not met, then the iterative process continues by exchanging investment and operation policies between the models.

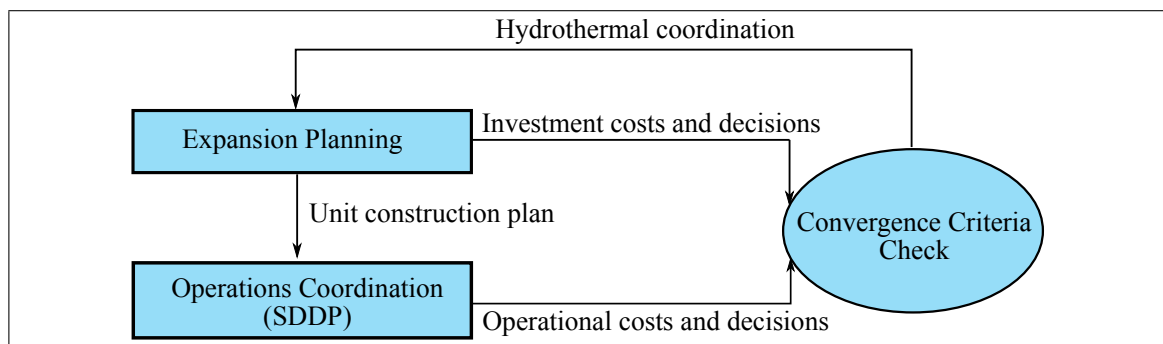


Figure 1.6. Iterative process diagram for EP with SDDP.

Despite being the conventional model for operations coordination, the SDDP methodology is not well suited to be incorporated into EP, because of the following reasons:

- (i) A global optimum is not guaranteed to be reached and there is a lack of bounding methods to quantify optimality gaps.

- (ii) Its use of load blocks impede the representation of relevant phenomena, as has been discussed in Section 1.3.1.
- (iii) Long setup and computation times of the iterative process may render it impractical for its use by a decision maker that aims to run several different case studies.

Therefore, there has been an effort to include reservoir management and inflow scenario trees in EP models without drawing on SDDP. The main difficulty of including endogenous inflow scenario trees in EP models is that the system's state is linked between time points—through reservoir water levels—, so including additional hydrological scenarios makes the problem size grow exponentially. This has led most work to adopt deterministic approaches and carry out optimizations for different individual hydro scenarios, which casts doubts on the performance of expansion plans obtained even with elaborate models, such as the one proposed by Khodaei et al. (2012). Moreover, EP models in literature consider hydrological basins in an aggregated way, grouping many generators together. This ignores the fact that cascaded water from upstream reservoirs can be used in multiple downstream generators to produce power, as well as ignores the difference in individual power plant water heads.

Embedded hydrological scenarios have been included in early research using SP to consider multiple seasonal water availability states in small systems (Sanghvi & Shavel, 1986). More recent work has focused on larger systems and multiple independent inflow scenarios that span throughout the many years of the operational horizon (Costa et al., 1990; Kenfack et al., 2001). Greater detail in uncertainty has been captured by Gil et al. (2015) via a scenario reduction methodology to obtain yearly inflow scenarios.

Nonetheless, all of these works use load blocks to represent operations, and thus ignore the phenomena described in Section 1.3.1. These methodologies could lead to investment plans that present problems or higher costs in their actual operations, given that a recent

operational study carried on the hydrothermal grid of Chile for high penetration of renewables concludes that “*the operational flexibility supplied by reservoir hydro power plants is indispensable to manage the intra-daily and hourly variability of net demand, reducing its impact on thermal plants*”(CDEC-SING, 2016)³. Additionally, models in literature avoid the exponential explosion of problem size by considering that no water storage is allowed between years. This way, operations are independent on a yearly basis because water levels are effectively reseted. This greatly simplifies the problem, but ignores the capability that many systems have of storing water in large reservoirs on an interannual basis to hedge against hydrological uncertainty.

1.4. Contributions

This work proposes an EP model that performs a centralized and simultaneous coordination of generation and transmission investments in hydrothermal systems. It is specially suited for systems with high penetration of volatile energy sources, since it captures chronology of operations on representative days with hourly resolution, which are chosen with a clustering technique. This allows to consider the concurrence of load and renewable profiles, to constrain generator ramps, and to model hourly reservoir management. Multiple investment periods and endogenous inflow uncertainty in the operational scale are considered. In contrast to previous works, inter-annual water storage is allowed within each multi-year period and operations consider an inflow scenario tree in each period, which provides a more accurate representation of hydrothermal coordination. Additionally, the water network is modeled in detail, so that spilled flows are cascaded and different hydraulic efficiencies are considered.

Another innovative aspect of the model is the consideration of a *nominal* long-term scenario, which is the most likely to happen, and several *extreme* long-term scenarios, which may have severe impacts on the system, such as a significant inflow reduction. Decisions in the investment scale must then hedge the risk of these events. This is achieved

³Independent System Operator.

by assigning near-zero probabilities to the extreme long-term scenarios, so that they do not affect the objective function of the model, but only further constrain its feasible region. This avoids the need of quantifying the probability of high impact events that are hard to predict. Total cost caps are implemented for each extreme long-term scenario, so the decision maker using this tool can set limits on the total cost he is willing to incur in each case.

In summary, the main contributions of this work are as follows:

- A new EP model for generation and transmission EP in hydrothermal systems is proposed, which uses representative days with hourly resolution and allows inter-annual water storage. Uncertainty in inflows is considered in the operational scale and, simultaneously, extreme long-term scenarios are considered in the investment scale.
- Numerical experiments are carried out and results highlight the need to consider intra-hourly phenomena in systems with high renewable penetration. The relevance of the intra-day flexibility that reservoir hydro power plants provide is illustrated. Additionally, the flexibility that inter-annual water storage provides is reported. Finally, it is also shown that small changes in the investment plan can better prepare the system for extreme long-term scenarios.

Additionally, the model is a Linear Program, which can be efficiently tackled by commercial solvers. The problem is solved through a scenario based decomposition technique called Progressive Hedging Algorithm (PHA) to achieve lower computation times for large scale systems. The algorithm is adapted so that scenarios with near-zero probabilities can be included without affecting numerical performance.

The rest of this document is organized as follows. The mathematical formulation of the proposed model is exhibited in Section 2. The scenario structure, components and solution method of the optimization problem are described in detail. Numerical experiments are reported in Section 3 for a dataset representing the Chilean power system. Conclusions are drawn on Section 4 and future work is outlined in Section 5.

2. MODEL FORMULATION AND SOLUTION METHOD

2.1. Scenario and Temporal Structure

This Section presents the scenario and decision structure over operational and investment timescales for the proposed EP model. Generation and transmission investment decisions are taken in every period and installed capacity is accumulated. Uncertainty unfolds throughout successive periods and is captured in *long-term scenarios*. Every period consists of multiple years in which operational decisions, such as power dispatch, transmission flows, water storage management, among others, are obtained for a number of representative days with hourly resolution. Uncertainty in the short term is captured by *inflow scenarios*. Fig. 2.1 shows the decision structure for one long-term scenario, where inflow scenarios unfold as branches from each investment node.

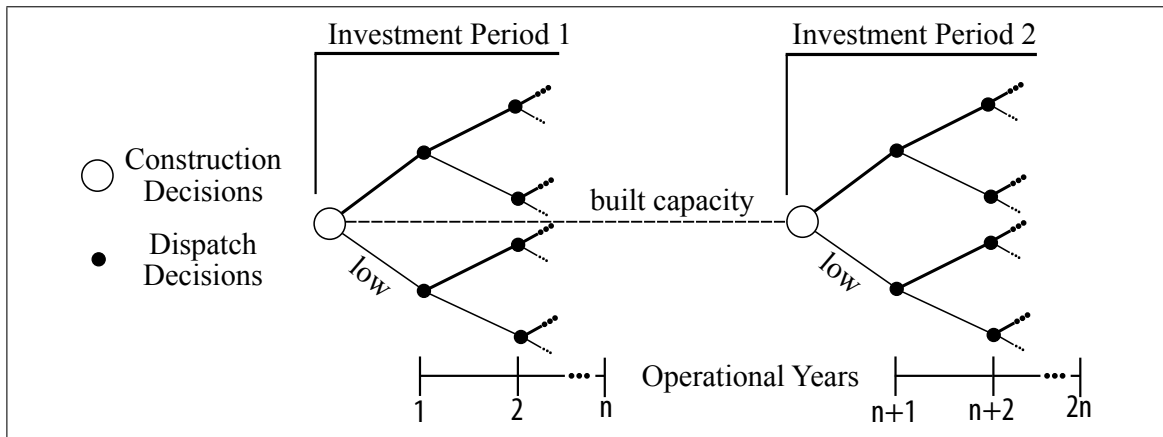


Figure 2.1. One long-term scenario structure with inflow scenario trees in each investment period.

Using water to generate power in hydroelectric plants implies no immediate marginal cost for the system, so a boundary condition must be set in order to prevent the excessive depletion of reservoirs. Previous works on hydrothermal EP set initial reservoir volumes on each year as parameters and constrain the model so water levels at the end of the year reach at least that value (e.g. see the works by Khodaei et al. (2012); Sanghvi & Shavel (1986); Costa et al. (1990); Kenfack et al. (2001); Gil et al. (2015)). In consequence,

reservoir levels are reseted on a yearly basis and flows that come into the system can only be stored and used within the same year.

Our model allows inter-annual storage in reservoirs by resetting water levels only after a multi-year investment period. Water is then allowed to be stored between several years and used in any of them. This better represents operations in hydrothermal systems, since dispatch decisions in each year must account for all possible scenarios that could follow. For example, in a year with high inflow availability a system operator would consider storing water for subsequent years to hedge against the risk of future low inflow availability. If the next year actually presents high inflow availability, then spillage or overflow of reservoirs is possible. The operator must then make a decision for operations in the first year that considers both possible futures. This is termed as *non-anticipativity* in SP, because decisions makers cannot exactly anticipate what is going to happen.

The proposed model is first formulated for only one long-term scenario, such as the one in Fig. 2.1. Section 2.2 outlines the notation and Section 2.3 presents and discusses the mathematical formulation. The model is then extended to accommodate multiple long-term scenarios in Section 2.4.

2.2. Notation Under One Long-Term Scenario

2.2.1. Sets and Indices

\mathcal{P}	Set of investment periods, indexed by p .
\mathcal{D}	Set of representative days, indexed by d .
\mathcal{H}	Set of hours, indexed by h .
\mathcal{H}_d	Set of hours in day d .
\mathcal{H}_p	Set of hours in period p .
\mathcal{S}	Set of inflow scenarios, indexed by s .
$\Gamma_{h,s}$	Set of inflow scenarios that follow the same trajectory as inflow scenario s up to hour h .

\mathcal{B}	Set of buses, indexed by b .
\mathcal{G}	Set of all generators, indexed by g .
\mathcal{G}_b	Set of generators located in bus b .
\mathcal{G}^H	Set of hydro generators.
\mathcal{L}	Set of transmission lines, indexed by ℓ .
\mathcal{L}_b^{in}	Set of transmission lines directed into bus b .
\mathcal{L}_b^{out}	Set of transmission lines directed out of bus b .
\mathcal{N}	Set of nodes in the water network, indexed by n .
\mathcal{N}^R	Set of water nodes that are reservoirs.
\mathcal{C}	Set of connections in the water network, indexed by c .
\mathcal{C}_n^{in}	Set of connections directed into water node n .
\mathcal{C}_n^{out}	Set of connections directed out of water node n .

2.2.2. Parameters Under One Long-Term Scenario

θ_h	Scaling factor of hour h . It is the number of hours that are represented by hour h in its year. It is numerically the same as the number of days that as represented by the day this hour belongs to.
y_p	Length of period p [years].
π_s	Probability of inflow scenario s in any given year.
f_p	Factor to bring costs in period p to present value.
$\phi_{g,p}^{Gfix}$	Annual fixed Operation & Maintenance (O&M) costs of generator g on period p [US\$/MW/year].
$\phi_{g,p}^{Ginv}$	Annualized investment costs of generator g on period p [US\$/MW/year].
$\phi_{\ell,p}^{Lfix}$	Annual fixed O&M costs of transmission line ℓ on period p [US\$/MW/year].
$\phi_{\ell,p}^{Linv}$	Annualized investment costs of transmission line ℓ on period p [US\$/MW/year].
ϕ_g^{OM}	Variable O&M costs of generator g [US\$/MWh].
$\phi_{g,p}^{fuel}$	Fuel cost of generator g on period p [US\$/MWh].
$l_{b,h}$	Demand load in bus b and hour h [MW].
η_ℓ^L	Transmission efficiency factor of line ℓ .

$c_{g,h}$	Maximum generating capacity factor for generator g in hour h as fraction of installed capacity.
$b_{g,p}^G$	Existing built capacity of generator g that will be operational in period p [MW].
$b_{\ell,p}^L$	Existing built capacity of transmission line ℓ that will be operational in period p [MW].
\overline{B}_g^G	Investment cap per period for generator g [MW].
\overline{B}_ℓ^L	Investment cap per period for line ℓ [MW].
\overline{C}_g^G	Upper bound on installed capacity for generator g [MW].
\overline{C}_ℓ^L	Upper bound on installed capacity for line ℓ [MW].
r_g^{up}	Upward ramping rate of generator g as fraction of installed capacity.
r_g^{dn}	Downward ramping rate of generator g as fraction of installed capacity.
$w_{n,h,s}$	Natural water inflow into node n at hour h and inflow scenario s [m ³ /h].
V_n^i	Initial stored water at each reservoir $n \in \mathcal{N}^R$ [m ³].
$\underline{V}_{n,h,s}$	Lower water volume storage limit for node n at hour h and inflow scenario s [m ³].
$\overline{V}_{n,h,s}$	Upper water volume storage limit for node n at hour h and inflow scenario s [m ³].
η_g^H	Hydraulic efficiency of generator $g \in G^h$ [MW/(m ³ /h)].

2.2.3. Variables Under One Long-Term Scenario

$B_{g,p}^G$	Capacity construction decision of generator g at period p [MW].
$B_{\ell,p}^L$	Capacity construction decision of line ℓ at period p [MW].
$C_{g,p}^G$	Cumulative capacity of generator g on period p [MW].
$C_{\ell,p}^L$	Cumulative capacity of line ℓ on period p [MW].
$P_{g,h,s}$	Dispatch level of generator g at hour h under inflow scenario s [MW].
$F_{\ell,h,s}$	Power flow through line ℓ at hour h under inflow scenario s [MW].
$D_{b,h,s}$	Power dumped in bus b at hour h under inflow scenario s [MW].
$W_{c,h,s}$	Water flow through connection c at hour h under inflow scenario s [m ³ /h].
$V_{n,h,s}$	Stored water volume in water node n at hour h under inflow scenario s [m ³].

2.3. Optimization Problem Under One Long-Term Scenario

Under each long-term scenario, the proposed optimization model is described by (2.1)–(2.15).

2.3.0.1. Objective Function

$$\begin{aligned}
 \min \quad & \sum_{p \in \mathcal{P}} f_p \left\{ \left[\sum_{g \in \mathcal{G}} C_{g,p}^G (\phi_{g,p}^{Gfix} + \phi_{g,p}^{Ginv}) \right. \right. \\
 & \left. \left. + \sum_{\ell \in \mathcal{L}} C_{\ell,p}^L (\phi_{\ell,p}^{Lfix} + \phi_{\ell,p}^{Linv}) \right] y_p \right. \\
 & \left. + \sum_{h \in \mathcal{H}_p} \sum_{s \in \mathcal{S}} \theta_h \pi_s \left[\sum_{g \in \mathcal{G}} P_{g,h,s} (\phi_g^{OM} + \phi_{g,p}^{fuel}) \right] \right\} \quad (2.1)
 \end{aligned}$$

The objective is to minimize total investment and expected operational costs over all inflow scenarios, which are calculated as in (2.1). Annualized investment and yearly fixed O&M costs are considered for generation and transmission capacity, which are multiplied by the number of years in each period. Variable O&M and fuel costs are calculated for power generation in each representative hour and inflow scenario, and are scaled up to the period and multiplied by its probability to calculate total expected costs. A factor is used to bring costs to present value and the amounts are summed up for all periods.

2.3.0.2. Power system operational constraints

$$l_{b,h} + \sum_{\ell \in \mathcal{L}_b^{out}} F_{\ell,h,s} + D_{b,h,s} = \sum_{g \in \mathcal{G}_b} P_{g,h,s} + \sum_{\ell \in \mathcal{L}_b^{in}} \eta_{\ell}^L F_{\ell,h,s} \quad \forall b \in \mathcal{B}, h \in \mathcal{H}, s \in \mathcal{S} \quad (2.2)$$

$$D_{b,h,s} \geq 0 \quad \forall b \in \mathcal{B}, h \in \mathcal{H}, s \in \mathcal{S} \quad (2.3)$$

The power balance constraint is expressed in (2.2). Load at each bus and hour must be satisfied by local generators and power imports from other buses for every inflow scenario. Excess power is allowed to be dumped at no cost and no loss of load is permitted, which is implied from (2.3). Transmission is represented by a transport model in which power flows may be routed in any direction, though imports in each bus are penalized by a constant efficiency factor. The extension to other transmission representations, such as DC power flow, are straightforward and can be accommodated in the model.

$$0 \leq F_{\ell,h,s} \leq C_{\ell,p}^L \quad \forall \ell \in \mathcal{L}, h \in \mathcal{H}_p, s \in \mathcal{S}, p \in \mathcal{P} \quad (2.4)$$

$$0 \leq P_{g,h,s} \leq C_{g,p}^G c_{g,h} \quad \forall g \in \mathcal{G}, h \in \mathcal{H}_p, s \in \mathcal{S}, p \in \mathcal{P} \quad (2.5)$$

Eq. (2.4) constrains transmission flow according to capacity. Generation dispatch levels are also limited by infrastructure, but by an hourly capacity factor as well, as shown in (2.5). For variable generators, $c_{g,h}$ represents the fraction of the installed capacity that can be dispatched according to the amount of renewable resource present in each hour. For other generators this parameter represents the average available capacity.

$$P_{g,h+1,s} - P_{g,h,s} \leq r_g^{up} C_{g,p}^G \quad \forall g \in \mathcal{G}, h \in \mathcal{H}_d, d \in \mathcal{D}, s \in \mathcal{S} \quad (2.6a)$$

$$P_{g,h,s} - P_{g,h+1,s} \leq r_g^{dn} C_{g,p}^G \quad \forall g \in \mathcal{G}, h \in \mathcal{H}_d, d \in \mathcal{D}, s \in \mathcal{S} \quad (2.6b)$$

The use of representative days with hourly resolution allows the implementation of ramping constraints (2.6a) and (2.6b). Ramp rates are regarded as fractions of the current installed capacity for each project. The hours of each day are considered in a circular manner, implying that dispatch in the last hour ramps to the first of the same day.

2.3.0.3. Power system construction constraints

$$C_{g,p}^G = b_{g,i}^G + \sum_{i=1}^{p-1} B_{g,i}^G \quad \forall g \in \mathcal{G}, p \in \mathcal{P} - \{1\} \quad (2.7)$$

$$C_{\ell,p}^L = b_{\ell,i}^L + \sum_{i=1}^{p-1} B_{\ell,i}^L \quad \forall \ell \in \mathcal{L}, p \in \mathcal{P} - \{1\} \quad (2.8)$$

Eqs. (2.7) and (2.8) show how cumulative installed capacity considers existing infrastructure plus new additions. Expansions that are decided on one period are considered to finish construction just before the start of the next period. Existing capacity, represented by $b_{g,i}^G$ and $b_{\ell,i}^L$, is specified on a period basis to account for capacity that is decommissioned after projects reach the end of their lifetimes.

$$0 \leq B_{g,p}^G \leq \overline{B}_g^G \quad \forall g \in \mathcal{G}, p \in \mathcal{P} \quad (2.9a)$$

$$0 \leq C_{g,p}^G \leq \overline{C}_g^G \quad \forall g \in \mathcal{G}, p \in \mathcal{P} \quad (2.9b)$$

$$0 \leq B_{\ell,p}^L \leq \overline{B}_\ell^L \quad \forall \ell \in \mathcal{L}, p \in \mathcal{P} \quad (2.10a)$$

$$0 \leq C_{\ell,p}^L \leq \overline{C}_\ell^L \quad \forall \ell \in \mathcal{L}, p \in \mathcal{P} \quad (2.10b)$$

Investment in each period is limited in (2.9a) and (2.10a) to reflect labor, resource or capital mobilization bounds. Additionally, cumulative capacities are capped in (2.9b) and (2.10b) to reflect resource and terrain availability, and other factors.

2.3.0.4. Hydraulic system constraints.

$$w_{n,h,s} + \sum_{c \in C_n^{in}} W_{c,h,s} + V_{n,h,s} = \sum_{c \in C_n^{out}} W_{c,h,s} + V_{n,h+1,s} \quad \forall n \in \mathcal{N}, h \in \mathcal{H}, s \in \mathcal{S} \quad (2.11)$$

The water network is composed of nodes, which receive natural inflows and can store water, and connections, which can transport water downstream between them. It is the equivalent of a common transportation graph, with nodes and edges. Conservation of mass at each node, hour and inflow scenario is enforced in (2.11), where the difference between inflows and outflows is reflected on an increase or decrease of stored water.

$$\underline{V}_{n,h,s} \leq V_{n,h,s} \leq \bar{V}_{n,h,s} \quad \forall n \in \mathcal{N}, h \in \mathcal{H}, s \in \mathcal{S} \quad (2.12)$$

Water volume storage at each node is constrained by (2.12) to reflect design and terrain limits, as well as regulatory requirements that vary between locations and time of year. Non reservoir nodes have no storage capability (i.e. $\underline{V}_{n,h,s}$ and $\bar{V}_{n,h,s}$ take a value of 0) and act merely as junctions.

$$V_n^i = V_{n,first(\mathcal{H}_p),s} \quad \forall n \in \mathcal{N}^R, p \in \mathcal{P}, s \in \mathcal{S} \quad (2.13a)$$

$$V_n^i \leq V_{n,last(\mathcal{H}_p),s} \quad \forall n \in \mathcal{N}^R, p \in \mathcal{P}, s \in \mathcal{S} \quad (2.13b)$$

Boundary conditions are relevant modeling decisions in problems with storage. To the best of our knowledge, all previous EP work with hydro has considered initial and final stored water volumes in a year as parameters, so operational years become independent intervals and water management is only allowed within that horizon (e.g. see Khodaei et al. (2012); Sanghvi & Shavel (1986); Costa et al. (1990); Kenfack et al. (2001); Gil et al. (2015)). This work extends the management horizon to a multi-year investment period. Constraint (2.13a) sets the water volume of reservoirs at the first hour of each period — $first(\mathcal{H}_p)$ — to given values. Constraint (2.13b) ensures that at least the initial water volume of each reservoir is reached at the last hour of each period — $last(\mathcal{H}_p)$ —, in order to avoid excessive usage.

$$P_{g,h,s}/\eta_g^H \leq W_{c,h,s} \quad \forall g \in \mathcal{G}^H, h \in \mathcal{H}, s \in \mathcal{S} \quad (2.14)$$

Eq. (2.14) shows how the power system and the water network are linked at hydroelectric generators, where water flows are used to produce electricity. We assume a constant

hydraulic efficiency to avoid non linearities in the problem. This simplification is widely used and has been shown by Gjelsvik et al. (2010) to present little error in medium term hydrothermal operations, even for reservoirs with significant head differences. Spilled water is cascaded downstream and can be used by other power plants.

$$V_{n,h,s} = V_{n,h,s'} \quad \forall n \in \mathcal{N}, s' \in \Gamma_{h,s}, h \in \mathcal{H}, s \in \mathcal{S} \quad (2.15)$$

In order to enforce non-anticipativity, Eq. (2.15) forces water storage decisions in every hour to be the same in all inflow scenarios that are indistinguishable up to that moment.

2.4. Extension to Multiple Long-Term Scenarios

The linear program outlined in (2.1)–(2.15) can be written in the following compact manner:

$$\min_{\mathbf{x}} \quad \sum_{p \in \mathcal{P}} \left[c_p^\top \mathbf{x}_p + \sum_{s \in \mathcal{S}} \pi_s Q(p, \mathbf{x}_p, s) \right] \quad (2.16a)$$

$$\text{s.t.} \quad D \mathbf{x} \geq e \quad (2.16b)$$

$$\text{where} \quad Q(p, \mathbf{x}_p, s) = \min_{\mathbf{y}_{p,s}} \quad d_p^\top \mathbf{y}_{p,s} \quad (2.17a)$$

$$\text{s.t.} \quad W \mathbf{y}_{p,s} \geq u_p - T \mathbf{x}_p \quad (2.17b)$$

Here, (2.16a) summarizes (2.1) by representing capacity decisions —variables C^L , C^G , B^L , B^G — in period p by the vector \mathbf{x}_p , their investment costs by c_p and their constraints (2.7)–(2.10b) by (2.16b). Operational costs in each inflow scenario and period are represented by the function Q , which reflects the total cost of dispatch decisions — P , F , D , W , V —, represented by the vector $\mathbf{y}_{p,s}$. In turn, (2.17b) condenses constraints (2.2)–(2.6b) and (2.11)–(2.15). The problem can then be generalized to accommodate multiple

long-term scenarios as follows.

$$\min_{\mathbf{x}} \sum_{\omega \in \Omega} \gamma_{\omega} \left(\sum_{p \in \mathcal{P}} \left[c_p^{\omega \top} \mathbf{x}_p^{\omega} + \sum_{s \in \mathcal{S}} \pi_s Q(p, \mathbf{x}_p^{\omega}, s, \omega) \right] \right) \quad (2.18a)$$

$$\text{s.t. } (\mathbf{x}_p^{\omega}, \mathbf{y}_{p,s}^{\omega}) \in \Delta_p^{\omega} \quad (2.18b)$$

$$\mathbf{x}_p^{\omega} = \mathbf{x}_p^{\omega'} \quad \forall \omega' \in \Psi_p^{\omega}, p \in \mathcal{P}, \omega \in \Omega \quad (2.18c)$$

Let the set of all long-term scenarios be Ω , indexed by ω , and their probabilities be γ_{ω} . The objective function of the multiple scenario extension can then be expressed as in (2.18a). If Δ_p is the space of all combinations of \mathbf{x}_p and $\mathbf{y}_{p,s}$ that satisfy constraints (2.16b) and (2.17b) in a given period p , then Δ_p^{ω} is the space of feasible combinations of \mathbf{x}_p^{ω} and $\mathbf{y}_{p,s}^{\omega}$ for long-term scenario ω , enforced in (2.18b). Different parameters and cost coefficients may be specified in each long-term scenario. Non-anticipativity is enforced in (2.18c), where construction decisions in each period are forced to be equal for all long-term scenarios that are indistinguishable up to that moment, gathered in the set Ψ_p^{ω} . Figure 2.2 illustrates a long-term scenario tree with 3 trajectories.

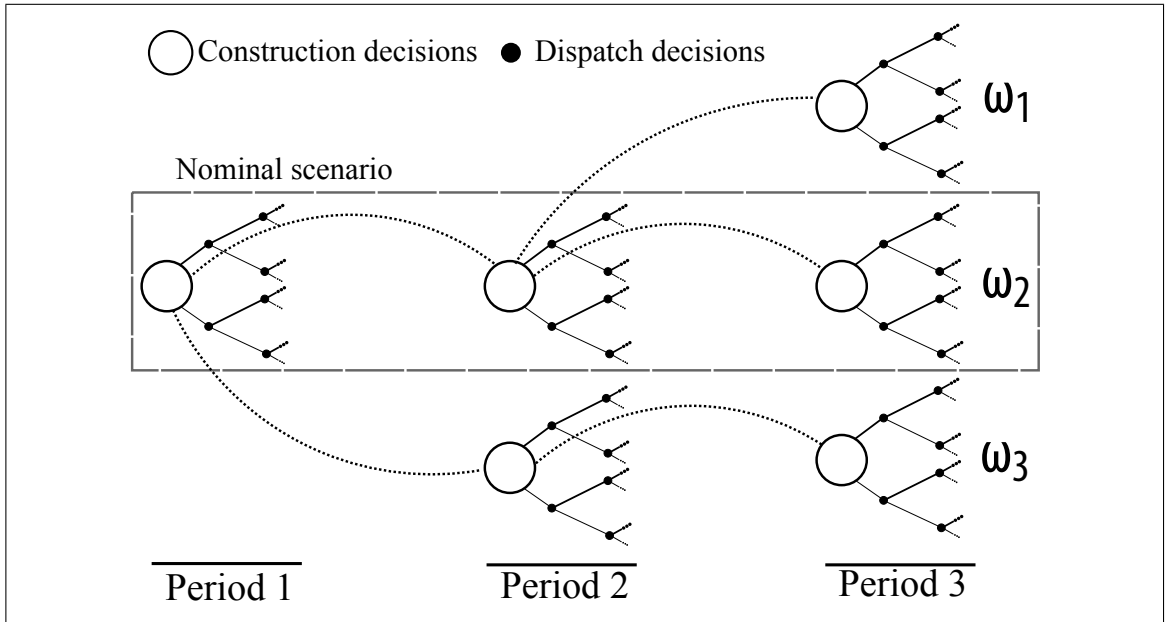


Figure 2.2. Long-term scenario tree structure with one nominal scenario and two extreme scenarios.

As discussed in Section 1.3.2, multiple works on EP formulate long-term scenario trees and assign probabilities according to different methods so that obtained investment plans have the least expected cost. However, assigning discrete probabilities to scenarios that span several decades where unfolding phenomena are not completely understood may become an insurmountable challenge.

This work captures long term uncertainty by minimizing investment and operations costs for an *nominal scenario* —highlighted in Fig. 2.2—, while also accounting for *extreme scenarios* that unfold in different periods. The probability of occurrence of the extreme scenarios is considered to be near-zero, so the optimization problem (2.18a)–(2.18c) ignores their costs. Hence, these extreme scenarios only add constraints to the problem so the system is prepared to meet the required load in a reliable manner in such cases. However, only considering feasibility in those long-term scenarios could result in investment plans which imply unacceptably high operational costs in the extreme scenarios. An upper bound on total cost — ϕ_ω^{cap} — for each long-term scenario is then implemented in the additional constraint (17d), in order to set the maximum cost the decision maker is willing to accept in extreme scenarios.

$$\sum_{p \in \mathcal{P}} \left[c_p^\omega \mathbf{x}_p^\omega + \sum_{s \in \mathcal{S}} \pi_s Q(p, \mathbf{x}_p^\omega, s, \omega) \right] \leq \phi_\omega^{\text{cap}} \quad \forall \omega \in \Omega \quad (17d)$$

2.5. Solution Method

The complete problem structure defined in (2.18a)–(17d) consists on several long-term scenarios linked by investment decisions. The problem is decomposed and solved using the Progressive Hedging Algorithm (PHA) first proposed by Rockafellar & Wets (1991). This method has received significant interest recently, because it can take advantage of modern parallel and distributed computing to reduce solution times for large problems. It has been successfully applied to power system problems, such as stochastic EP that considers variability of load and renewable output profiles (Muñoz & Watson, 2015), and

medium term hydrothermal operations scheduling (Dos Santos et al., 2009). Advanced schemes have focused on reducing solution time by adaptively changing algorithm parameters throughout its execution (Zéphyr et al., 2014), and establishing lower bound computation methods to be able to calculate an optimality gap (Gade et al., 2016).

Algorithm 1 gives an overview on the PHA, where $f(\mathbf{x})$ represents the objective function in (2.16a). It is an augmented Lagrangian method that decomposes the problem on a long-term scenario basis by relaxing the non-anticipativity constraint (2.18c). The objective function of each long-term scenario subproblem is then augmented with penalizing factors that steer each solution toward a non-anticipative optimum.

Algorithm 1 Progressive Hedging

- 1: $i \leftarrow 0, \quad \text{gap} \leftarrow \infty$
 - 2: $\mathbf{w}_i^\omega \leftarrow \mathbf{0} \quad \forall \omega \in \Omega$
 - 3: $\mathbf{x}_i^\omega \leftarrow \operatorname{argmin}_{\mathbf{x}} [f(\mathbf{x}_i^\omega)]$
s.t. [(2.16b) – (2.17b)]
 - 4: **while** $\text{gap} \geq \epsilon$ **do**
 - 5: $\bar{\mathbf{x}}_i \leftarrow \sum_{\omega \in \Omega} \gamma^\omega \mathbf{x}_i^\omega$
 - 6: $i \leftarrow i + 1$
 - 7: $\mathbf{w}_i^\omega \leftarrow \mathbf{w}_{i-1}^\omega + \boldsymbol{\rho}^\top (\mathbf{x}_{i-1}^\omega - \bar{\mathbf{x}}_{i-1}) \quad \forall \omega \in \Omega$
 - 8: $\mathbf{x}_i^\omega \leftarrow \operatorname{argmin}_{\mathbf{x}} [f(\mathbf{x}_i^\omega) + \mathbf{w}_i^{\omega\top} \mathbf{x}_i^\omega + \frac{1}{2} \boldsymbol{\rho}^\top \|\mathbf{x}_i^\omega - \bar{\mathbf{x}}_i\|^2]$
s.t. [(2.16b) – (2.17b)]
 - 9: $\text{gap} \leftarrow \sum_{\omega \in \Omega} \|\mathbf{x}_i^\omega - \bar{\mathbf{x}}_i\|^2$
-

The proposed model does not include costs on extreme long-term scenarios in the objective function of the problem and only consider them for reliability enforcement. However, the PHA cannot be directly applied to a problem that has scenarios with null probabilities. Instead, these extreme scenarios are assigned minuscule probabilities so that their costs fall within the optimality gap of the applied solver software. However, this raises a problem for the PHA.

Having scenarios with probabilities that range orders of magnitude in difference increases solving time significantly, because the weighted averaged value of a variable calculated in Line 5 in each iteration will result in a value excessively close to that of the

scenario with high probability. In consequence, penalization factors for the nominal long-term scenario calculated on Line 7 will be light. This causes variable values in the nominal scenario to change by only a small amount in each iteration, so a great number of iterations are needed for convergence.

An alternative formulation drawn from Birge & Louveaux (1997) is implemented, which is also proven to achieve convergence and optimality for convex problems. Instead of calculating a variable value average weighted by the scenario probabilities, Line 5 can be replaced by a simple arithmetic average as shown in (2.19). To maintain the proof of convergence to the optimum, the penalty factor for all variables must be multiplied by the inverse of the probability of their scenario. Line 7 in the original algorithm can then be replaced by (2.20). This formulation allows convergence in a reasonable number of iterations in this application.

$$\bar{\mathbf{x}}_i \leftarrow \frac{\sum_{\omega \in \Omega} \mathbf{x}_i^\omega}{|\Omega|} \quad (2.19)$$

$$\mathbf{w}_i^\omega \leftarrow \mathbf{w}_{i-1}^\omega + \frac{1}{\gamma^\omega} \boldsymbol{\rho}^\top (\mathbf{x}_{i-1}^\omega - \bar{\mathbf{x}}_{i-1}) \quad \forall \omega \in \Omega \quad (2.20)$$

3. IMPLEMENTATION AND COMPUTATIONAL EXPERIMENTS

3.1. Problem Data and Setup

The proposed model was implemented by developing new modules in the open source SWITCH platform, which is a planning tool based in Python/Pyomo and publicly available¹. The problems are solved with the Gurobi 7.0 solver using the Barrier Method with a 0.01% duality gap on an Intel Xeon E5-2620 24-core machine with 32 GB of RAM memory.

Case studies comprise 10 two-year investment periods spanning from 2020 to 2039 on the future interconnected power system of Chile. As of 2016, it consisted on two separate systems that served an aggregate 71.68 TWh per year with nearly 20 GW of installed capacity. Bus load and renewable generator profiles were constructed from actual 2015 data. Future load was projected using estimated load growth rates. Existing and proposed generator and transmission line characteristics were obtained from Comisión Nacional de Energía (2016a,b) and reduced to a total of 68 aggregated existing and new generators and 23 transmission lines that connect 20 buses. The technologies used by these projects are described in Table 3.1.

Transmission line investment costs consider a constant overnight cost per unit of distance and power. This represents the incremental cost of longer lines and more robust structures and conductors, and results in an investment cost curve illustrated on Fig. 3.1 as the *linear cost function*. Nonetheless, investment costs in transmission lines exhibit a behavior more similar to that of the *quadratic cost function* illustrated in the same Figure, since there are significant economies of scale in their construction. In this work, the proposed model uses a linear cost function to avoid non-linearities in the optimization problem. This represents a reasonable approximation of costs as long as resulting investment in capacity is sufficiently small or large.

¹The online public repository where the SWITCH model is published can be found at: <https://github.com/switch-model/switch>.

Table 3.1. Generator technologies with average characteristics.

Technology	Projects	Fuel	Overnight Cost [US\$/kW]	Fixed O&M Cost [US\$/kW]	Average Fuel Cost in 2020 [US\$/MWh]	Ramp Rate [fraction of capacity]
Hydro RoR	8	—	3100	50	—	1.0
Hydro Series	5	—	3400	14	—	1.0
Hydro Reservoir	12	—	3100	14	—	1.0
Wind	11	—	2100	40	—	1.0
Solar PV	9	—	1950	25	—	1.0
OCGT	6	Diesel	946	8	200	0.5
CCGT	5	Gas	1100	14	89	0.3
ICE	5	Diesel	910	30	166	1.0
ST	7	Coal	3000	35	41	0.0

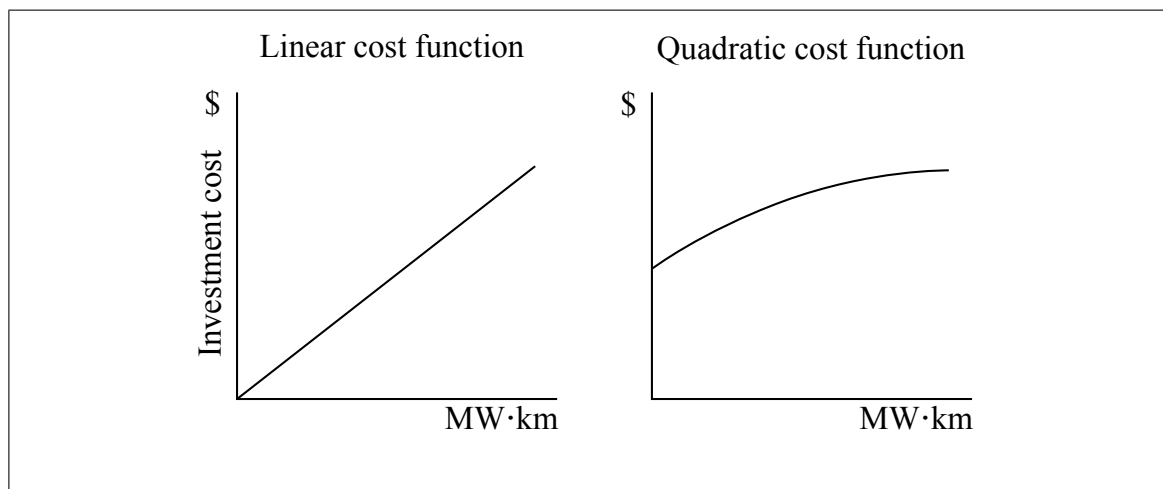


Figure 3.1. Schematic investment cost functions for transmission projects.

Hydroelectric projects include units that can store water (Reservoir), units located downstream from them that use cascading flows (Series), and run-of-river projects (RoR). The main water basins are schematically represented in Fig. 3.2 with their water network.

The remaining sets of input data can be found in Appendix A, and both the model and its input files are available upon e-mail request to the author².

²E-mail address: bmaluend@uc.cl

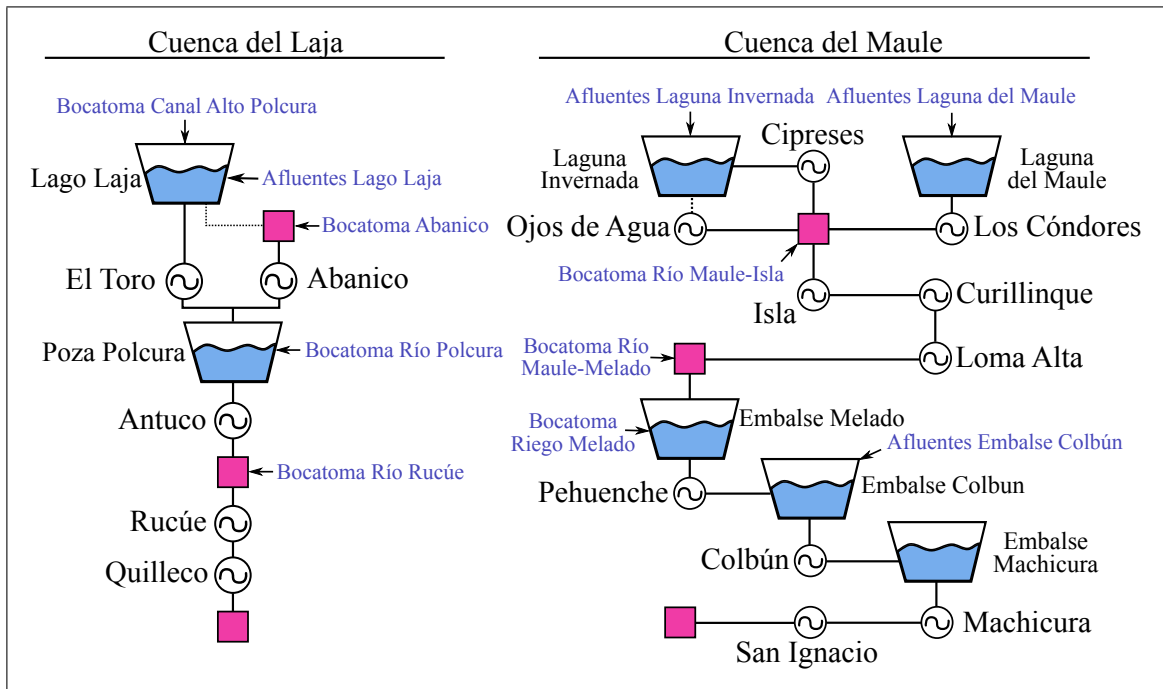


Figure 3.2. Schematic of water networks in the two most relevant hydraulic basins of Chile.

Section 3.2 reports two experiments on the hydrothermal model for one long-term scenario defined by (2.1)–(2.15). The sampling of representative days and inflow scenarios that are used in the experiments is outlined in Section 3.2.1. A comparison of the investment plans obtained when using load blocks and representative hourly days is performed in Section 3.2.2 and the effect of inter annual water storage is explored in Section 3.2.3. Long term uncertainty is considered in Section 3.2.4 through several long-term scenarios, where the PHA is used to solve the problem.

3.2. One Long-Term Scenario Hydrothermal Model

3.2.1. Representative Operational Days and Inflow Scenarios

To formulate inflow scenarios for these case studies, hydrological series need to be understood. A study by Aravena & Gil (2015) states that hydrological timeseries in Chile present little autocorrelation, so each year's hydrology can be assumed independent of

previous years. In addition, inflow records are used as a distribution from which to sample possible scenarios. In consequence, careful sampling of hydrologies may allow capturing most of the effects of inflow uncertainty, while reducing the problem size considerably.

The *hierarchical clustering* methodology was used to sample inflow scenarios, where all possible occurrences are grouped into clusters that exhibit similar characteristics. A representative scenario is then selected for each group. The similarity of timeseries is usually calculated through a measure of distance. In this work, the *Dynamic Time Warping* distance was used as the measuring metric. This method has shown to be the most adequate when comparing timeseries, since it measures similarity of shape as well as magnitude (Liao, 2005). The 56 current historical records (1960-2015) were clustered into 3 representative years using hierarchical clustering and Dynamic Time Warping as a distance metric. The representative inflow scenario for each cluster was taken to be the hydrology for which the cluster's variance in respect to it was the minimum. Fig. 3.3 exhibits the historical hydrologies clusters and the representative years highlighted in red.

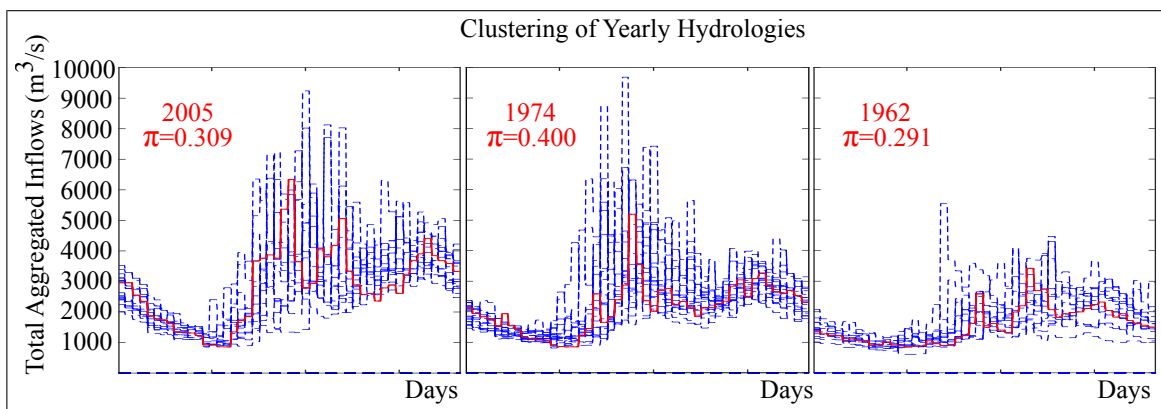


Figure 3.3. Hydrologies clustered into 3 groups, with representative year highlighted.

Scenario trees were then constructed by combination resulting in 9 different trajectories for each 2-year period. An additional inflow scenario with null probability is added to each period to enforce reliability, which is the worst registered hydrology—the year

1998— multiplied by a factor of 0.8. This replaces the need for capacity reserve constraints present in other EP models. The resulting scenario tree can be observed in Fig. 3.4, where only the first 3 periods of the simulation are exhibited.

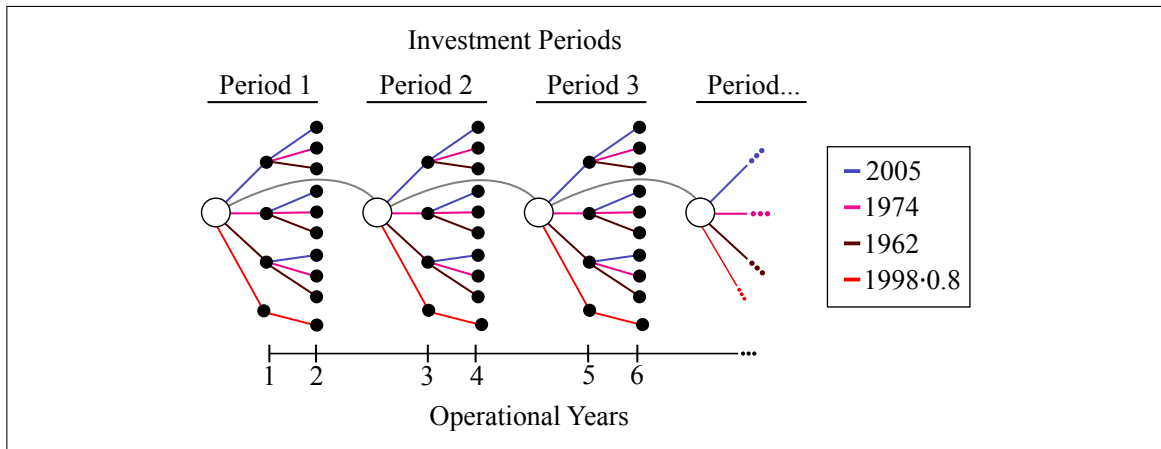


Figure 3.4. Inflow scenario structure for one long-term scenario.

Representative days were chosen by the same methodology of hierarchical clustering based on the Dynamic Time Warping distance metric, sampling from actual aggregated daily net load curves from the Chilean system on the year 2015. The 10% of days with the most abrupt evening ramps were clustered together and the remaining 90% were clustered into 3 samples. As with inflow scenarios, the representative day from each cluster was then chosen as the one which minimized the variance of the cluster around it. The use of 4 representative days implied a total of 96 hours per year. The chosen dates and their weights —the amount of days in their cluster— are highlighted in Fig. 3.5, where the clusters of daily net load curves are exhibited.

3.2.2. Case Study 1: Hourly Resolution Versus Load Blocks

The effect of time resolution is examined by comparing the outputs of a model that considers representative days with hourly resolution —the *RD model*— with those of an equivalent model that considers monthly load blocks —the *LB model*—. The RD model is completely described by (2.1)–(2.15). The LB model is analogous, though hours are

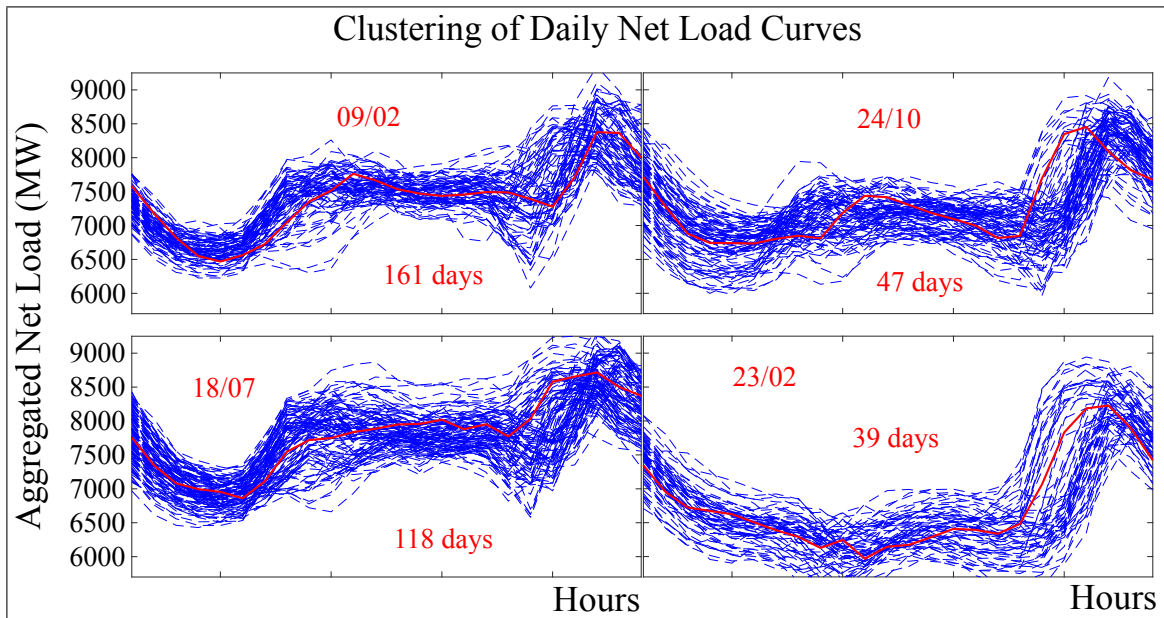


Figure 3.5. Aggregated daily net load curves grouped in 4 clusters with representative date highlighted.

replaced by load blocks, ramping constraints (2.6a)–(2.6b) are ignored and water storage is balanced on a monthly instead of hourly in (2.11). Inflows, renewable resource availability and load profiles were discretized into 8 blocks per month to be inputted in the LB model, for a total of 96 blocks per year that matches the number of hours in the RD model.

In order to compare the LB and RD models for different levels of flexibility in the system, each model is run with three different portfolios of new must-build reservoir hydro power plants equivalent to 3.75 G, 2.5 GW, and 0 GW of new capacity. Investment plans for the 2.5 GW case can be observed in Fig. 3.6.

The LB model delivers a construction plan with more investment on PV and Run-of-River projects when compared with the RD model, which builds more combined cycle units. This reflects the fact that the LB model averages renewable resource and load profiles—as described in Section 1.3.1—and thus “flattens” the fine granularity differences that can be captured hourly. The LB model invests on additional diesel open cycle units, but dispatches them infrequently on the main inflow scenarios, because they are

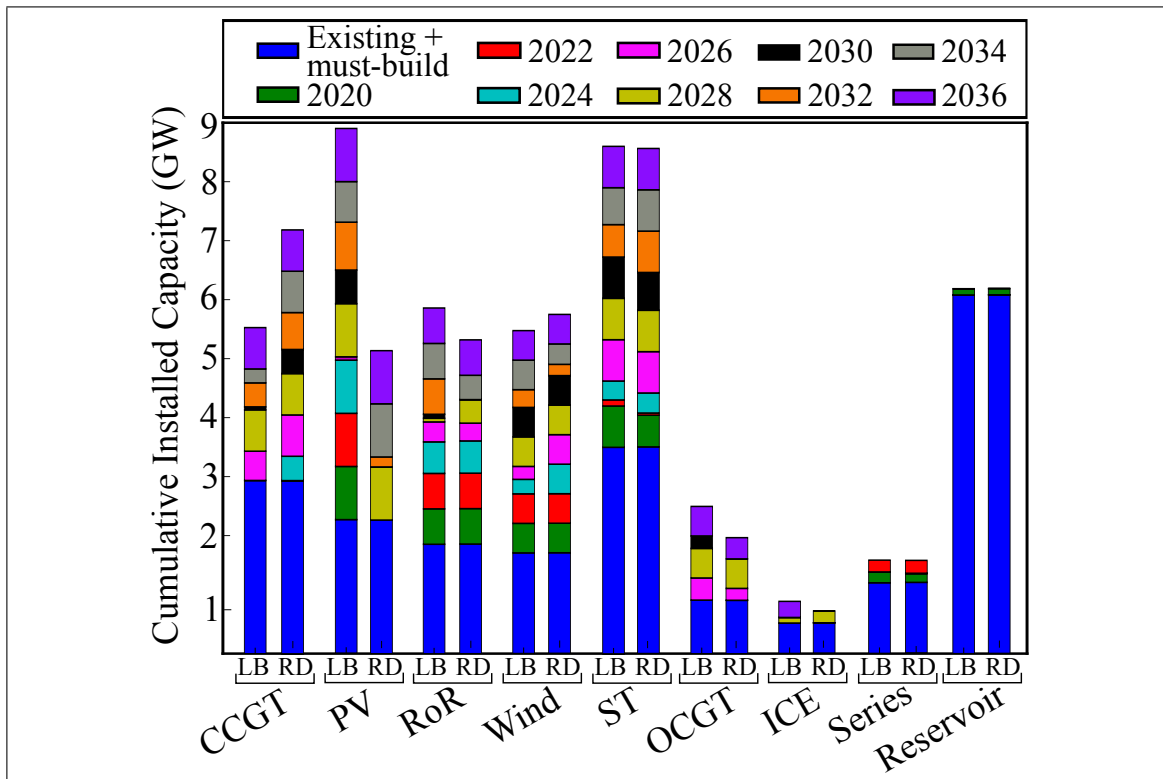


Figure 3.6. Generation investment plans yielded by the LB and RD models for 2.5 GW of must-build reservoir hydro new capacity.

built to provide sufficient capacity for the drought scenario. This contrasts with the use of combined cycle capacity both to provide energy and power sufficiency in the hourly formulation.

These results indicate that the use of load blocks in EP models will provide investment plans with a higher amount of renewable capacity in comparison with the use of representative days. This must be taken into account by decision makers when performing EP by either method.

For further analysis, the operational performance of the investment plans obtained by the LB and RD models are assessed using an economic dispatch model with ramping constraints, spanning all the hours of the 2022-2039 horizon and all inflow scenarios in each period. This experiment allows comparing the performance of both methods of sampling and representing time in EP models. Whereas an economic dispatch with ramping

constraints lacks some constraints that a full unit commitment formulation may have, it adequately represents real operations cost for comparing two expansion plans.

To implement this test, the model described by (2.1)–(2.15) is ran by fixing the variables $B_{g,p}^G$ and $B_{\ell,p}^L$ to the values of each investment plan. It is possible that some investment plan is not able to supply all demand in every hour and scenario, so load is allowed to be curtailed at a fixed cost. Unserved load is represented by the non-negative variable $U_{b,h,s}$ defined for all buses, hours and inflow scenarios, and its cost is symbolized by ϕ^{UL} . Eqs. (2.1) and (2.2) then change to Eqs. (3.1) and (3.2) for this experiment, respectively. The parameter ϕ^{UL} is set at a fixed value of 500 US\$/MWh.

$$\min \sum_{p \in \mathcal{P}} f_p \left\{ \sum_{h \in \mathcal{H}_p} \sum_{s \in \mathcal{S}} \theta_h \pi_s \left[\sum_{b \in \mathcal{B}} U_{b,h,s} \phi^{UL} + \sum_{g \in \mathcal{G}} P_{g,h,s} (\phi_g^{OM} + \phi_{g,p}^{fuel}) \right] \right\} \quad (3.1)$$

$$l_{b,h} + \sum_{\ell \in \mathcal{L}_b^{out}} F_{\ell,h,s} + D_{b,h,s} = U_{b,h,s} + \sum_{g \in \mathcal{G}_b} P_{g,h,s} + \sum_{\ell \in \mathcal{L}_b^{in}} \eta_{\ell}^L F_{\ell,h,s} \quad \forall b \in \mathcal{B}, h \in \mathcal{H}, s \in \mathcal{S} \quad (3.2)$$

Cost results for the 2.5 GW level of must-build new hydro capacity are exhibited in Fig. 3.7. It can be observed that the construction plan resulting from the LB model has a higher investment cost, because of the greater construction of renewable power plants. This greater renewable resource capacity allows the LB model to incur in less operational costs than the RD model, which invests less on infrastructure, but incurs in higher operational costs. Nevertheless, the total cumulative costs (i.e. total investment costs plus the operational costs up until each period) are always lower for the RD model plan. The present value of the total investment and operations costs for the LB model is 3.3% higher than for the RD model when their investment plans are operated on all of the hours in the studied horizon.

Besides costs, the reliability and efficiency of an investment plan is relevant as well. The amount of unserved load can be taken as a measure of reliability, for it indicates the capability of a construction plan of serving load both in terms of energy and of power.

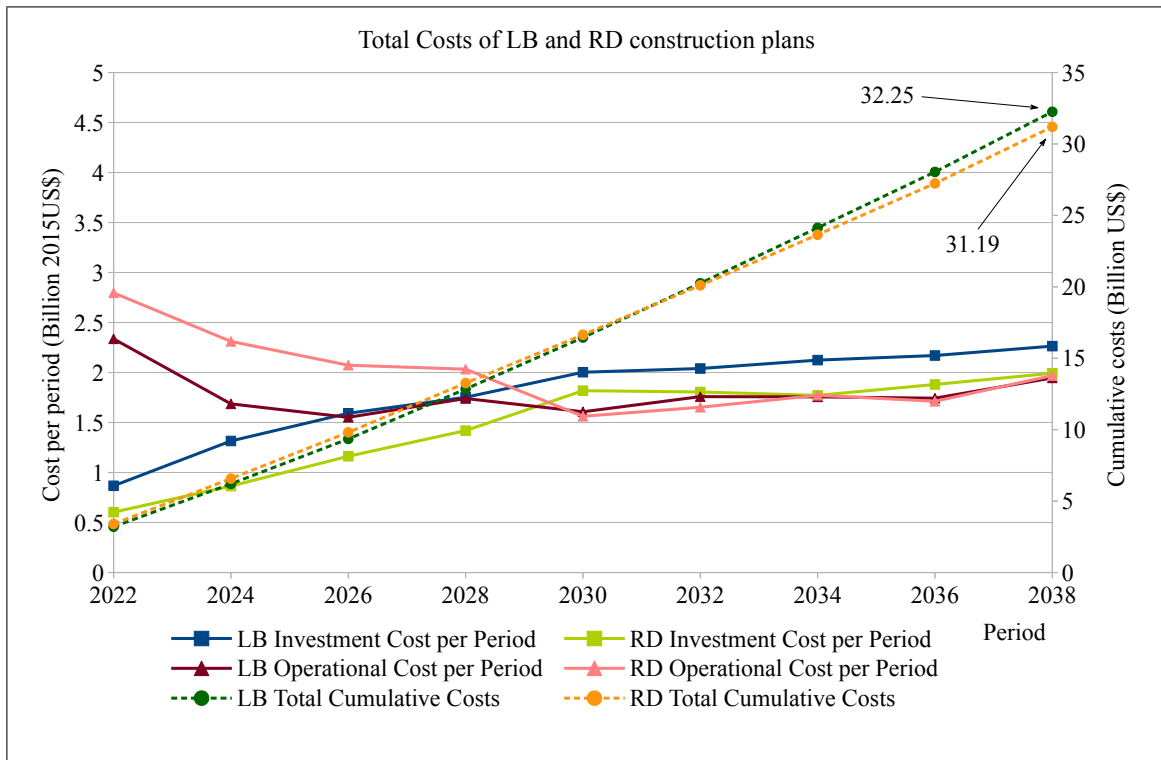


Figure 3.7. Expected costs for the production costing simulations of the investment plans generated by the LB and RD models for the 2.5 GW new hydro case.

The efficiency of the system may be considered as the capability of making good use of the infrastructure. Hence, the amount of *dumped* energy should be examined to determine how much of the electricity generation is being wasted. Fig. 3.8 reports the comparison of both these variables when operations are run on the LB and the RD models. Reported magnitudes are expected values over all 9 inflow scenarios in each period.

It can be observed that the investment plan produced by the LB model performs worse in both reliability and efficiency metrics. Whereas the RD model plan leaves almost no load unserved, the LB system increasingly fails to provide energy to all consumers as more renewable capacity is built, up to more than 1% per period. This is caused by the inability of the generation mix to provide enough controlled ramping capacity. The amount of dumped energy behaves similarly, since as more renewable capacity is built by the LB model, increasing amounts of energy is curtailed. Generation simply occurs in moments

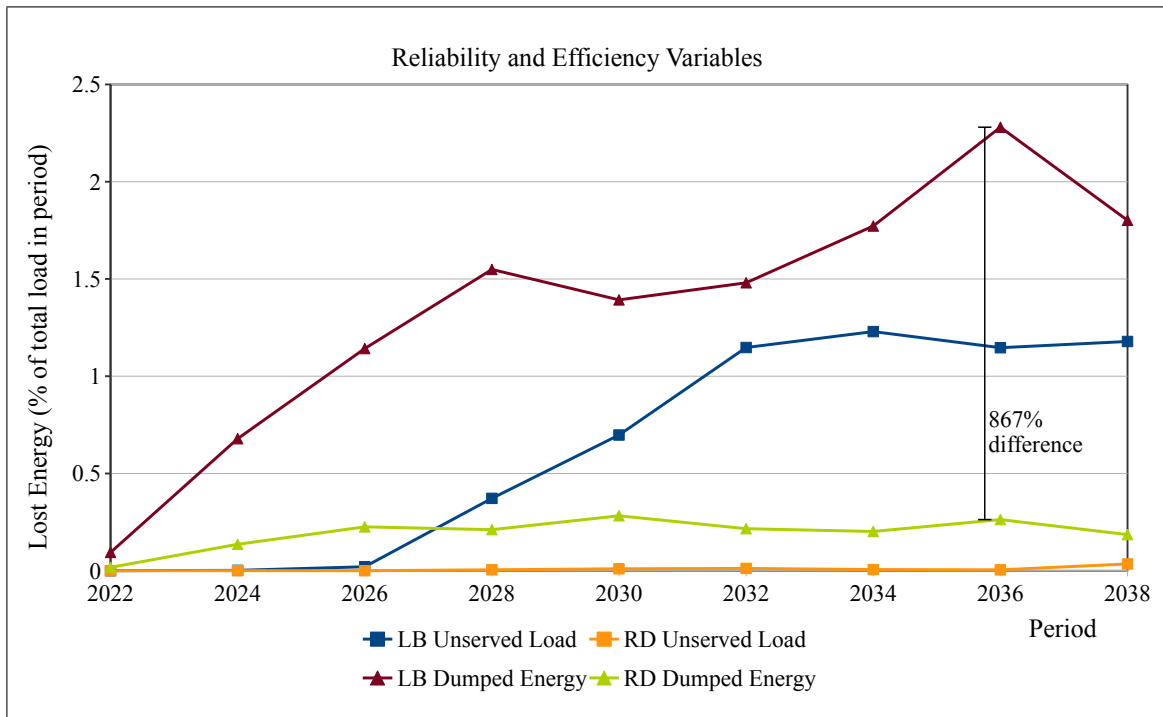


Figure 3.8. Comparison of expected dumped energy and unserved load in production costing simulations of the investment plans rendered by the RD and LB models.

when there is not enough demand and energy is lost up to more than 2% per period. Differences reach their peak at the 2036 period, when the LB construction plan dumps more than 8 times as much as the RD plan.

Cost and operational metrics for all levels of must-build hydro capacity are summarized in Table 3.2. It can be observed that the investment plan produced by the RD model yields between 1.88% and 3.38% smaller total costs (investment and operation) than the LB plan depending on the amount of must-build hydro power. Moreover, curtailed energy throughout the operational horizon can reach up to 1.96% of total generation with the LB plan when no new reservoir hydro plants are built. Similarly, unserved load when operating the LB investment plan increases as new hydro capacity diminishes. These results show that representative days offer a better representation of operational conditions than load blocks, given their ability to capture intra-day flexibility requirements. In addition,

the differences between the two approaches are more apparent when the amount of new reservoir hydro capacity is lower. This highlights the role of hydro power as a relevant source of intra-day flexibility to accommodate high levels of renewables.

Table 3.2. Total Cost and Operational metrics of LB and RD investment plans

Must-build Hydro (GW)	Total Cost (Billion 2015US\$)			Unserved Load (%)		Curtailed Energy (%)	
	LB	RD	$\Delta\%$	LB	RD	LB	RD
0	35.63	34.98	1.88	0.72	0.02	1.96	0.12
2.5	32.25	31.20	3.38	0.73	0.01	1.45	0.20
3.75	30.75	29.86	2.98	0.68	0.00	1.32	0.32

This experiment shows that the use of load blocks to represent load and time in EP models overestimates the amount of renewable capacity that is economic and reliable to incorporate, even for flexible hydrothermal systems. The use of representative days with hourly resolution better captures flexibility requirements in a system with volatile resources.

3.2.3. Case Study 2: Effects of Inter-annual Storage

As previously discussed, proposed hydrothermal EP models in literature allow water storage and use exclusively within each year (e.g. see the work by Khodaei et al. (2012); Sanghvi & Shavel (1986); Costa et al. (1990); Kenfack et al. (2001); Gil et al. (2015)). To explore the potential benefits of allowing this feature, the results obtained when using the model described in Section 2.3 and a variation where no inter-annual storage is allowed are compared. Additionally, the effect of non-anticipativity constraints in the resulting investment plan is explored through the use of another variation of the model.

The first formulation is termed the *Intra-annual model* (IA) and only allows water storage on a yearly basis. The non-anticipativity constraint expressed in (2.15) is not applied, since operational decisions in one year are independent from other years. Constraints (2.13a) and (2.13b), which enforce boundary conditions, are then applied on a

yearly basis instead of per period. The second formulation is named *Inter-annual model with perfect foresight* (PF) and allows water storage over multiple years throughout each inflow scenario, but ignores the non-anticipativity constraint (2.15). Finally, the full model described by (2.1)–(2.15) is tested and termed *Inter-annual model with non-anticipativity* (NA). Several optimizations are carried out varying the applied discount rate used to calculate the factor f_p that brings costs to present value. This allows comparing not only the magnitude of costs, but also the timing of investment costs incurred on by each formulation. Results are reported in Table 3.3.

Table 3.3. Total investment costs (Billion 2015US\$)

Discount rate	NA	IA		PF	
0%	37.63	38.27	+1.69%	37.61	-0.07%
2%	46.25	46.92	+1.46%	46.24	-0.01%
4%	37.67	38.25	+1.56%	37.69	+0.06%
7%	28.06	28.50	+1.56%	28.05	-0.04%
10%	21.07	21.47	+1.87%	21.07	-0.02%
12%	17.56	17.91	+2.00%	17.55	-0.01%
14%	14.70	14.99	+2.03%	14.69	-0.03%

Table 3.4. Average wall clock time per process (s).

	Inter-annual with non-anticipativity	Intra-annual	Inter-annual with perfect foresight
Instantiation	704.8	194.1	692.3
Solve	298.6	119.9	296.9
Total	1003.4	314.0	989.2

Present value of all investment costs incurred on by each formulation is presented in Table 3.3 for several discount rates. The Intra-annual model incurs in 1.56% higher investment costs than the Inter-annual model with non-anticipativity when the discount rate is set at its nominal value of 7%. As the value of this parameter increases, cost differences increase to up to 2.03%. Results show that this is caused by the timing of constructions. Capacity addition decisions are similar, but slightly shifted in time. The earlier investments by the IA model arise from the need for more capacity on dry years,

whereas the other models can store water on high inflow availability years to use it on drier years and, thus, delay the need for new units as load increases. Examination of the investment plans rendered by the IA and the NA and PF models show that the former builds more combined cycle units than the latter, which build more open cycle plants that are used sporadically to complement hydro power during net load peaks.

Results also indicate that enforcing non-anticipativity in operations does not imply significantly different optimal investment plans. The PF model operates infrastructure in a more efficient way and generally needs less investment than the NA model, though the difference in cost did not surpass 0.1% for any of the studied cases. Nonetheless, this results are specific to the studied dataset and may not hold for other problem setups. Increasing the number of inflow scenarios, the reservoir capacity of the system and the number of years per period are factors that could increase the relevance of non-anticipativity in dispatch decisions and increase the differences between investment plans obtained by these two model formulations.

Table 3.4 shows wall clock timings for model instantiation and solution processes for each formulation. Reported solve times include wall clock time spent passing the instance to the solver and receiving results after the optimization. Solver time for the PF model is roughly the same as for the full NA model. Both these formulations take 3–4 times longer total time to be solved than the IA model. A trade-off then exists between conservativeness of water storage and solution time of the model.

3.2.4. Case Study 3: Robustness of the Expansion Plan

The PHA described in Section 2.5 is implemented by modifying the open source PySP stochastic programming module of the Pyomo package. As in Sections 3.2.2 and 3.2.3, the Barrier Method is used to solve the optimization problems, though the optimality gap is relaxed to 0.1% to achieve lower computation times. Near-zero probabilities for extreme long-term scenarios are set to $\gamma = 10^{-4}$, so their cost is practically ignored in the expected value minimization. The modified PHA requires that penalty factors ρ associated with

extreme scenarios' variables be amplified by a factor of 10^4 , to maintain the convergence proof. The algorithm is set to stop at a maximum of 12 iterations or when the convergence metric \mathbf{x}^c calculated in (3.3) is equal to or less than 1200 MW. The metric \mathbf{x}^c is the sum of difference between all variables in all scenarios with respect to the average value, so a lower value indicates that scenario variables are converging.

$$\mathbf{x}^c = \sum_{\omega \in \Omega} \sum_{i \in I} |\mathbf{x}_i^\omega - \bar{\mathbf{x}}_i| \quad (3.3)$$

Various ρ setting strategies are tested for convergence and speed by Watson & Woodruff (2011). Our work adopts the *cost proportional* strategy, where ρ values are equal to the cost coefficients in the objective function of each variable, scaled by a constant factor. Numerical tests were carried out to determine constant scale factors that produced better convergence and lower computational times.

Five extreme long-term scenarios are considered, named EXT1 through EXT5, whose effects are the same, but diverge from the nominal scenario in different periods. The long-term scenario tree structure can be observed in Fig. 3.9, where the period in which the effects of each extreme scenario begin is pictured. The parameter changes that are applied in each of said scenarios are the following.

- **Fuel costs** are increased by 25%.
- **Overnight costs** for fossil fueled generators are increased by 25%.
- **Water inflows** are reduced by 50%.

Equation (17d) in Section 2.4 establishes cost caps for each extreme long-term scenario, in order to avoid total cost spikes due to the small probabilities assigned. Several optimizations are carried out considering different caps to assess the impact of the long-term scenario tree upon the investment plan decided in the nominal scenario. To determine meaningful caps for this analysis, lower and upper bounds (ϕ_ω^{\min} and ϕ_ω^{\max}) are calculated

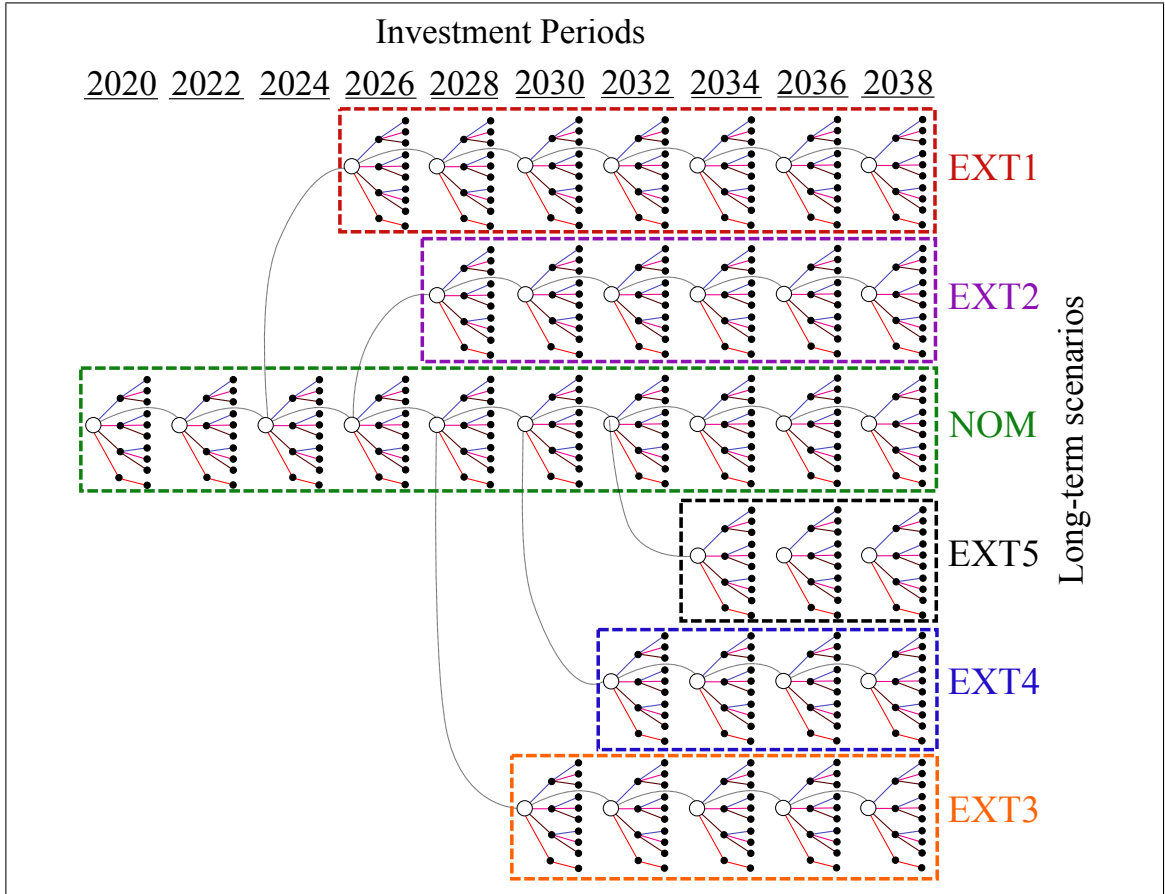


Figure 3.9. Tree diagram of long-term nominal and extreme scenarios.

for each long-term scenario. The lower bounds ϕ_{ω}^{\min} are obtained by calculating the optimal planning and operations for each scenario ω deterministically. The upper bounds ϕ_{ω}^{\max} are obtained by calculating the optimal operations in each scenario ω using the investment plan of the nominal long-term scenario, which is the equivalent of ignoring the long-term scenario in the planning process. Cost caps for each scenario are calculated as a linear combination of both bounds through different values of λ in (3.4). The lower and upper bounds of all extreme scenarios can be found in Table 3.5.

$$\phi_{\omega}^{\text{cap}} = \lambda \phi_{\omega}^{\min} + (1 - \lambda) \phi_{\omega}^{\max} \quad \forall \omega \in \Omega \quad (3.4)$$

For every proposed value of λ , the problem is solved through both an Extensive Formulation (EF) and through the proposed PHA. This allows benchmarking performance

Table 3.5. Total cost bounds (Billion 2015 US\$) for each extreme long-term scenario.

Scenario	Lower Bound (ϕ_{ω}^{\min})	Upper Bound (ϕ_{ω}^{\max})
EXT1	40.85	45.09
EXT2	38.99	43.11
EXT3	37.29	39.95
EXT4	35.43	37.30
EXT5	33.68	34.85

parameters of the decomposition algorithm against the “brute force” optimization method. In order to capture the potential computational advantages of problem decomposition and distributed computation, each problem and subproblem is allowed to be solved using only 4 computer cores. So, the 6 scenarios portrayed in Figure 3.9 can be solved in parallel in each iteration of the PHA using the 24 available cores of the workstation, whereas the full EF problem is solved in only 4. This experimental setup represents the common situation where no large computer server is available, but several medium-sized ones are.

The total costs of the nominal long-term scenario under various values of λ is reported in Figure 3.10 for both solution methods. Another metric of interest is total solver wall clock time taken by each method, which is displayed in Figure 3.11.

Figure 3.10 shows total costs in the nominal scenario, which are on average 1.47% higher when obtained through the PHA than with the EF. This is due to termination of the decomposition algorithm once the convergence criterion is met. If this criterion was to be made stricter, the objective function value would be closer to that of the EF, though solving time would increase. For λ values less than 0.25, the PHA was not able to meet the convergence criterion within the 12 maximum iterations. In those cases, objective function values are lower than the optimal values obtained through the EF, because the average solution at that moment is not admissible on all scenarios. Given enough iterations, the algorithm should converge upon the optimal solution. Nonetheless, experiments with a

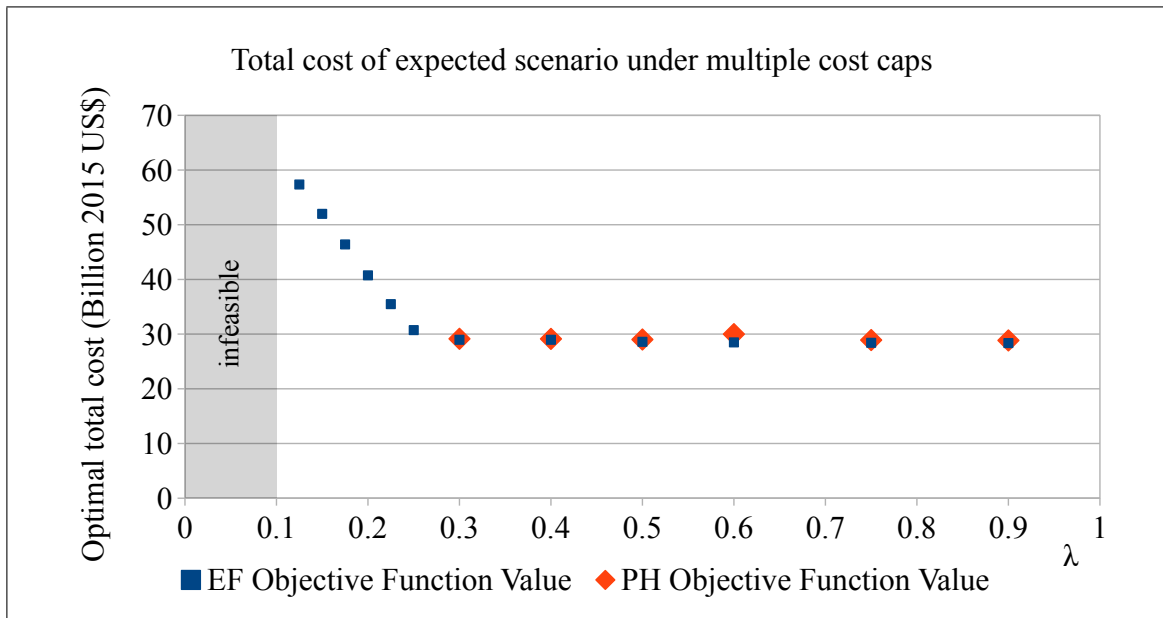


Figure 3.10. Total costs of the nominal long-term scenario under different cost caps for each extreme scenario.

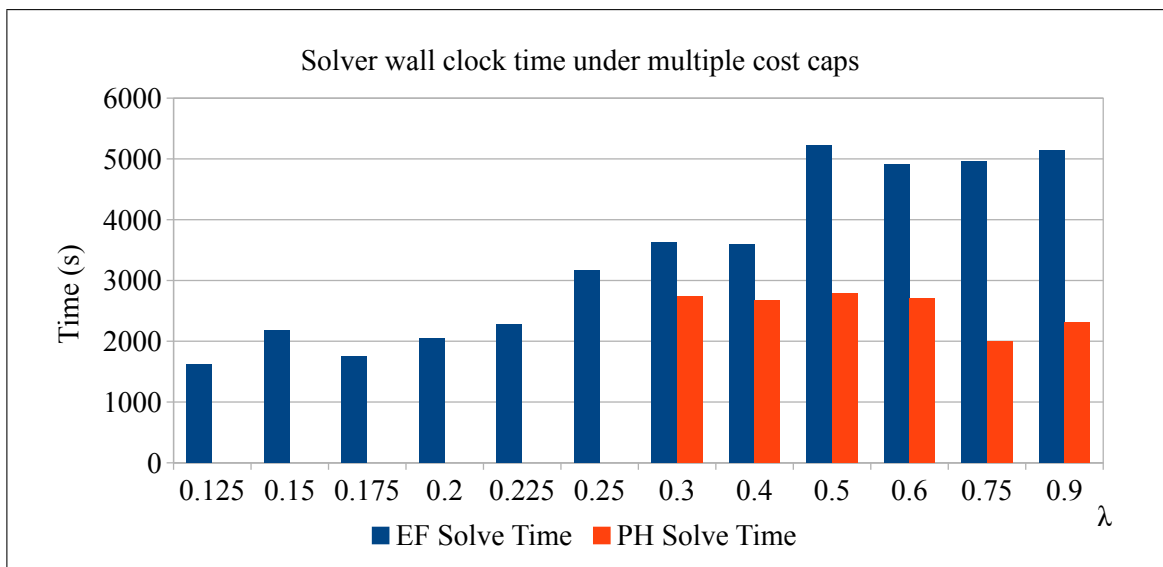


Figure 3.11. Solver wall clock time under different cost caps for each extreme long-term scenario.

significantly higher number of maximum iterations failed to converge on a reasonable amount of time and, thus, are excluded from the reported data.

The curve that is generated by joining the data points in Figure 3.10 is relevant, since it shows that 75% of the costs that the system would incur in, if extreme scenarios are ignored and actually take place, can be avoided with minimal additional investments. Relatively small changes in construction decisions allow hedging against most of the risk. The remaining 25% is shown to be expensive to hedge against, given the high increase in the slope of the cost curve. For a λ value of 0.1 the problem becomes unfeasible, since the cost caps are so strict that they cannot be met simultaneously in all scenarios.

A comparison between solving times using the EF and the PHA is reported in Figure 3.11. These experiments were carried out in a single machine by restricting the use of processor cores, but it allows assessing the potential of distributed computation when no large computer server is available, but several medium ones are. For all values of λ where the PHA meets the convergence criterion within the specified maximum number of iterations, it requires less solver wall clock time than the EF. This difference increases as λ does. Nevertheless, the time difference is reduced for lower values of λ , whereas the solution obtained by the PHA may even become unfeasible because of early optimization termination. Thus, when cost caps are strict, the PHA does not offer advantages, and when caps are relaxed, the decomposition technique speeds up solving time significantly with low cost objective value differences in comparison with the EF.

4. CONCLUSIONS

The challenge of evaluating how much renewable energy can be integrated in power systems in an economic and reliable manner can be met with the development of new planning tools. These should allow better assessment of flexibility and robustness requirements and can provide key insights to decision makers for the development of policies and investment plans.

A novel expansion planning model that can handle large-scale integration of volatile energy sources for hydrothermal grids has been presented. Operations are represented with an hourly resolution using selected representative days, the water network is explicitly modeled, and inflow uncertainty is endogenously accounted for.

The model is tested through numerical experiments on the power system of Chile. Model characteristics are highlighted and key indicators are benchmarked against conventional models found in the literature. A first case study shows that the use of representative days with hourly resolution, in contrast to traditional discrete load blocks, produces more flexible investment plans. The system performs better both in terms of economic and reliability metrics, such as dumped energy and loss of load. In addition, the proposed model highlights the significant role of reservoir hydro power in providing intra-day flexibility.

A second set of experiments illustrates the capability of reservoirs for hedging the system against inflow uncertainty by storing water throughout successive years. Results indicate that extending the storage horizon generates less conservative investment plans that shift some investments into the future and that build more peaking units and less baseload capacity. Nonetheless, solution times are increased, implying a trade-off. Another obtained insight is that enforcing non-anticipativity in operational decisions practically does not change the optimal investment plan.

Several extreme long-term scenarios with near-zero probability were considered in a third case study, where the problem is solved through the Progressive Hedging Algorithm.

A key insight obtained from the results is that the investment cost increase to hedge the system against risk of extreme scenarios follows a piecewise linear curve. Small changes in the nominal investment plan hedge against most of the long-term risk, but the remainder requires significantly more investments. Regarding optimization time, a trade off was identified. When cost caps are relaxed, the PHA requires significantly less solution time than the Extensive Form, but as the caps become more strict, the decomposition algorithm fails to converge within the maximum iteration limit.

The literature review and the case studies carried out in this work both highlight the need to further enhance investment and operational models with features that support assessing high-resolution chronological flexibility requirements. In a new paradigm of large-scale integration of volatile generation resources, it is key to incorporate greater detail of operations in planning activities. This allows a better evaluation of the amount of renewable energy that can be economically and reliably built and operated, and a better understanding on how other technologies, such as reservoir hydro power, can provide a suitable complement to achieve the goal of cleaner and economic grids.

5. FUTURE WORK

The presented work was implemented by extensively extending the capabilities of the open-source Python-based SWITCH model. Some features, such as the hydroelectric network modeling and code efficiencies, have already been pushed to the public repository in which SWITCH is maintained. Curating, documenting and publishing other developed new features are pending tasks. This will allow access to them by any member of the academy, industry and civil society, in the hopes of encouraging further discussion on the power systems of the future and on how to decarbonize the grid.

REFERENCES

- Abgottspon, H., & Andersson, G. (2016). Multi-horizon modeling in hydro power planning. *Energy Procedia*, 87, 2 - 10.
- Alizadeh, B., & Jadid, S. (2011, September). Reliability constrained coordination of generation and transmission expansion planning in power systems using mixed integer programming. *IET Generation, Transmission Distribution*, 5(9), 948-960.
- Aravena, I., & Gil, E. (2015). Hydrological scenario reduction for stochastic optimization in hydrothermal power systems. *Applied Stochastic Models in Business and Industry*, 31(2), 231–240.
- Barati, F., Seifi, H., Sepasian, M. S., Nateghi, A., Shafie-khah, M., & Catalão, J. P. S. (2015, Sept). Multi-period integrated framework of generation, transmission, and natural gas grid expansion planning for large-scale systems. *IEEE Transactions on Power Systems*, 30(5), 2527-2537.
- Birge, J. R., & Louveaux, F. (1997). *Introduction to stochastic programming*. New York: Springer.
- Campodónico, N., Binato, S., Pereira, M., & Mayak, F. (2003). *Expansion planning of generation and interconnections under uncertainty*. (3rd Balkans Power Conference)
- CDEC-SING. (2016). *Flexibilidad y sistemas de almacenamiento en el sistema eléctrico nacional en el año 2021*.
- Comisión Nacional de Energía. (2016a). *Fijación de precios de nudo de corto plazo de abril: Sistema interconectado central*. Santiago, Chile.
- Comisión Nacional de Energía. (2016b). *Fijación de precios de nudo de corto plazo de abril: Sistema interconectado del norte grande*. Santiago, Chile.

Costa, J., Campodónico, N., Gorenstin, B., & Pereira, M. (1990, August). A model for optimal energy expansion in interconnected hydrosystems. *Proceedings of the Tenth Power Systems Computation Conference*, 40-47.

Dehghan, S., Amjady, N., & Conejo, A. J. (2016, May). Reliability-constrained robust power system expansion planning. *IEEE Transactions on Power Systems*, 31(3), 2383-2392.

Dehghan, S., Amjady, N., & Kazemi, A. (2014, March). Two-stage robust generation expansion planning: A mixed integer linear programming model. *IEEE Transactions on Power Systems*, 29(2), 584-597.

Dos Santos, M. L., da Silva, E. L., Finardi, E. C., & Gonçalves, R. E. (2009). Practical aspects in solving the medium-term operation planning problem of hydrothermal power systems by using the progressive hedging method. *International Journal of Electrical Power & Energy Systems*, 31(9), 546 - 552.

Feng, Y., & Ryan, S. M. (2013). Scenario construction and reduction applied to stochastic power generation expansion planning. *Computers & Operations Research*, 40(1), 9 - 23.

Gade, D., Hackebeil, G., Ryan, S. M., Watson, J.-P., Wets, R. J.-B., & Woodruff, D. L. (2016). Obtaining lower bounds from the progressive hedging algorithm for stochastic mixed-integer programs. *Mathematical Programming*, 157(1), 47–67.

Gil, E., Aravena, I., & Cárdenas, R. (2015, July). Generation capacity expansion planning under hydro uncertainty using stochastic mixed integer programming and scenario reduction. *IEEE Transactions on Power Systems*, 30(4), 1838-1847.

Gjelsvik, A., Mo, B., & Haugstad, A. (2010). Long- and medium-term operations planning and stochastic modeling in hydro-dominated power systems based on stochastic dual dynamic programming. In *Handbook of power systems i* (1st ed., pp. 33–55). Springer Berlin.

Hemmati, R., Hooshmand, R. A., & Khodabakhshian, A. (2013, Sept). Comprehensive review of generation and transmission expansion planning. *IET Generation, Transmission Distribution*, 7(9), 955-964.

International Energy Agency. (2016). *World Energy Outlook*.

Jin, S., Botterud, A., & Ryan, S. M. (2014, Sept). Temporal versus stochastic granularity in thermal generation capacity planning with wind power. *IEEE Transactions on Power Systems*, 29(5), 2033-2041.

Jonghe, C. D., Hobbs, B. F., & Belmans, R. (2012, May). Optimal generation mix with short-term demand response and wind penetration. *IEEE Transactions on Power Systems*, 27(2), 830-839.

Kagiannas, A. G., Askounis, D. T., & Psarras, J. (2004). Power generation planning: a survey from monopoly to competition. *International Journal of Electrical Power and Energy Systems*, 26(6), 413 - 421.

Kenfack, F., Guinet, A., & Ngundam, J. M. (2001). Investment planning for electricity generation expansion in a hydro dominated environment. *International Journal of Energy Research*, 25(10), 927-937.

Khodaei, A., Shahidehpour, M., Wu, L., & Li, Z. (2012, Nov). Coordination of short-term operation constraints in multi-area expansion planning. *IEEE Transactions on Power Systems*, 27(4), 2242-2250.

Li, S., Coit, D. W., & Felder, F. (2016). Stochastic optimization for electric power generation expansion planning with discrete climate change scenarios. *Electric Power Systems Research*, 140, 401 - 412.

Liao, T. W. (2005). Clustering of time series data: a survey. *Pattern Recognition*, 38(11), 1857 - 1874.

- Massé, P., & Gibrat, R. (1957). Application of linear programming to investments in the electric power industry. *Management Science*, 3(2), 149-166.
- Motamedi, A., Zareipour, H., Buygi, M. O., & Rosehart, W. D. (2010, Nov). A transmission planning framework considering future generation expansions in electricity markets. *IEEE Transactions on Power Systems*, 25(4), 1987-1995.
- Muñoz, F. D., & Watson, J.-P. (2015). A scalable solution framework for stochastic transmission and generation planning problems. *Computational Management Science*, 12(4), 491–518.
- Nelson, J., Johnston, J., Mileva, A., Fripp, M., Hoffman, I., Petros-Good, A., . . . Kammen, D. M. (2012). High-resolution modeling of the western north american power system demonstrates low-cost and low-carbon futures. *Energy Policy*, 43, 436–447.
- Oliveira, G. C., Binato, S., & Pereira, M. V. F. (2007, Nov). Value-based transmission expansion planning of hydrothermal systems under uncertainty. *IEEE Transactions on Power Systems*, 22(4), 1429-1435.
- Palmintier, B. S., & Webster, M. D. (2016, April). Impact of operational flexibility on electricity generation planning with renewable and carbon targets. *IEEE Transactions on Sustainable Energy*, 7(2), 672-684.
- Park, H., & Baldick, R. (2015, March). Stochastic generation capacity expansion planning reducing greenhouse gas emissions. *IEEE Transactions on Power Systems*, 30(2), 1026-1034.
- Pereira, M. V. F., & Pinto, L. M. V. G. (1991). Multi-stage stochastic optimization applied to energy planning. *Mathematical Programming*, 52(1), 359–375.
- Pozo, D., Sauma, E., & Contreras, J. (2013, Feb). A three-level static milp model for generation and transmission expansion planning. *IEEE Transactions on Power Systems*, 28(1), 202-210.

Rockafellar, R. T., & Wets, R. J.-B. (1991, February). Scenarios and policy aggregation in optimization under uncertainty. *Math. Oper. Res.*, *16*(1), 119–147.

Sanghvi, A. P., & Shavel, I. H. (1986, May). Investment planning for hydro-thermal power system expansion: Stochastic programming employing the dantzig-wolfe decomposition principle. *IEEE Transactions on Power Systems*, *1*(2), 115-121.

Seifi, H., & Sepasian, M. S. (2011). *Electric power system planning: Issues, algorithms and solutions*. Springer Berlin Heidelberg.

van Stiphout, A., Vos, K. D., & Deconinck, G. (2017, Jan). The impact of operating reserves on investment planning of renewable power systems. *IEEE Trans. Power Syst.*, *32*(1), 378-388.

Velasquez, C., Watts, D., Rudnick, H., & Bustos, C. (2016, July). A framework for transmission expansion planning: A complex problem clouded by uncertainty. *IEEE Power and Energy Magazine*, *14*(4), 20-29.

Vinasco, G., Tejada, D., Silva, E. D., & Rider, M. (2014, May). Transmission network expansion planning for the colombian electrical system: Connecting the ituango hydro-electric power plant. *Electric Power Systems Research*, *110*, 94-103.

Watson, J.-P., & Woodruff, D. L. (2011). Progressive hedging innovations for a class of stochastic mixed-integer resource allocation problems. *Computational Management Science*, *8*(4), 355–370.

Wogrin, S., Galbally, D., & Reneses, J. (2016, July). Optimizing storage operations in medium- and long-term power system models. *IEEE Transactions on Power Systems*, *31*(4), 3129-3138.

Zéphyr, L., Lang, P., & Lamond, B. F. (2014). Adaptive monitoring of the progressive hedging penalty for reservoir systems management. *Energy Systems*, *5*(2), 307–322.

APPENDICES

APPENDIX A. INPUT DATA

Table A.1. Generation technologies.

Generation Technology	Project Lifetime (Years)	Energy Source	Scheduled Outage Rate	Forced Outage Rate	Maximum Built Capacity (MW)
Combined Cycle Gas Turbine (CCGT)	25	Gas	0.08	0.026	700
Steam Turbine (ST)	30	Coal	0.1	0.033	700
Internal Combustion Engine (ICE)	20	Diesel	0.05	0.05	400
Hydroelectric Reservoir	80	Water	0.094	0.051	3000
Hydroelectric Run-of-river	40	Water	0.04	0.03	600
Hydroelectric in Series	40	Water	0.05	0.051	800
Open Cycle Gas Turbine (OCGT)	25	Diesel	0.08	0.04	500
Solar PV	25	Solar	0	0.02	900
Wind Turbines	25	Wind	0.01	0.02	500

Table A.2. Generators.

Generator	Generation Technology	Bus	ϕ^{OM} (US\$/MWh)	Heat rate (MBTU/MWh)	$\overline{B^G}$ (MW)	η^H	Existing Capacity (MW) Year
CCGT_Alto_Jahuel	CCGT	Alto_Jahuel	3.85	7.13	740		340 1997
CCGT_Ancoa	CCGT	Ancoa	6	7	1200		0 -
CCGT_Encuentro	CCGT	Encuentro	6.37	6.86	1200		400 2001
CCGT_Mejillones	CCGT	Mejillones	4.03	7.34	2100		1200 2004
CCGT_Quillota	CCGT	Quillota	7.45	6.95	2200		1000 2002
Machicura_Signacio	Hydro Reservoir	Ancoa	0		132	0.512	132 1985
Los_Condores	Hydro Reservoir	Ancoa	0		150	6.000	150 2018
Colbun	Hydro Reservoir	Ancoa	0		472.8	1.429	473 1985
Pehuenche	Hydro Reservoir	Ancoa	0		568.3	1.667	568 1991
Cipreses	Hydro Reservoir	Ancoa	0		105.8	2.786	106 1995
Pangue	Hydro Reservoir	Charrua	0		465.8	0.885	466 1996
El_Toro	Hydro Reservoir	Charrua	0		448.7	4.740	449 1973

Ralco_Palmucho	Hydro Reservoir	Charrua	0		689	1.590	689	2004
Hydro_Charrua	Hydro Reservoir	Charrua	0		1500	1.920	1500	2029
Rapel	Hydro Reservoir	Rapel	0		376.6	0.674	377	1968
Hydro.Pto_Montt	Hydro Reservoir	Pto_Montt	0		1000	1.550	1000	2023
Canutillar	Hydro Reservoir	Pto_Montt	0		171.6	1.920	172	1990
RoR_Alto_Jahuel	Hydro RoR	Alto_Jahuel	0		544.2	2.777	544	2011
RoR_Ancoa	Hydro RoR	Ancoa	0		1000	0.839	173	2015
RoR_Charrua	Hydro RoR	Charrua	0		1000	1.448	360	2015
RoR_Itahue	Hydro RoR	Itahue	0		900	2.608	418	2015
RoR_Polpaico	Hydro RoR	Polpaico	0		600	4.030	177	2008
RoR.Pto_Montt	Hydro RoR	Pto_Montt	0		1000	0.629	20	2014
RoR.Quillota	Hydro RoR	Quillota	0		200	1.900	40	1989
RoR.Temuco	Hydro RoR	Temuco	0		900	0.724	129	2015
Isla_Curi_LAlta	Hydro Series	Ancoa	0		202	2.270	202	1997
Angostura	Hydro Series	Charrua	0		316	0.450	316	2014
Antuco	Hydro Series	Charrua	0		319.2	1.630	319	1981
Abanico	Hydro Series	Charrua	0		114.1	1.270	114	1959
Rucue.Quilleco	Hydro Series	Charrua	0		249	1.880	249	1998
ICE_Itahue	ICE	Itahue	22.20	7.93	94		47	2008
ICE.Lagunas	ICE	Lagunas	9.00	12.00	93.6		47	1991
ICE.Los_Vilos	ICE	Los_Vilos	27.00	8.72	248.2		124	2008
ICE.PdAzucar	ICE	PdAzucar	28.00	8.72	350		175	2007
ICE.Pto_Montt	ICE	Pto_Montt	28.00	8.72	250		125	2007
OCGT_Alto_Jahuel	OCGT	Alto_Jahuel	2.80	10.53	300		150	2004
OCGT.Cardones	OCGT	Cardones	24.40	9.50	1200		126	2000
OCGT_Charrua	OCGT	Charrua	3.50	10.30	600		250	2007

OCGT_DdAlmagro	OCGT	DdAlmagro	16.10	10.30	520	196	2005
OCGT_Hualpen	OCGT	Hualpen	6.00	12.00	600	88	2004
OCGT_Quillota	OCGT	Quillota	5.14	9.52	250	100	1994
PV_Alto_Jahuel	Solar PV	Alto_Jahuel	0		800	0	-
PV_Cardones	Solar PV	Cardones	0		1500	434	2015
PV_Encuentro	Solar PV	Encuentro	0		1200	660	2015
PV_DdAlmagro	Solar PV	DdAlmagro	0		1200	441	2015
PV_Laberinto	Solar PV	Laberinto	0		1000	220	2016
PV_Lagunas	Solar PV	Lagunas	0		1500	64	2015
PV_Maitencillo	Solar PV	Maitencillo	0		1200	300	2015
PV_PdAzucar	Solar PV	PdAzucar	0		1000	0	-
PV_Polpaico	Solar PV	Polpaico	0		1000	150	2016
ST_Ancoa	ST	Ancoa	3.37	9.8	1500	0	-
ST_Encuentro	ST	Encuentro	2.09	11.22	1425	625	1990
ST_DdAlmagro	ST	DdAlmagro	3.37	9.80	1000	0	-
ST_Hualpen	ST	Hualpen	4.21	9.89	1000	780	2007
ST_Maitencillo	ST	Maitencillo	1.63	9.02	1200	650	1999
ST_Mejillones	ST	Mejillones	4.92	9.82	1000	700	2007
ST_Nogales	ST	Nogales	4.02	9.97	1000	750	2009
Wind_Cardones	Wind	Cardones	0		700	0	-
Wind_Charrua	Wind	Charrua	0		800	155	2015
Wind_Encuentro	Wind	Encuentro	0		800	210	2015
Wind_DdAlmagro	Wind	DdAlmagro	0		700	284	2015
Wind_Hualpen	Wind	Hualpen	0		800	30	2015
Wind_Los_Vilos	Wind	Los_Vilos	0		1000	168	2015
Wind_Maitencillo	Wind	Maitencillo	0		700	301	2015
Wind_Rapel	Wind	Rapel	0		400	18	2015
Wind_PdAzucar	Wind	PdAzucar	0		800	442	2015
Wind_Polpaico	Wind	Polpaico	0		800	0	-
Wind_Pto_Montt	Wind	Pto_Montt	0		800	101	2015

Table A.3. Fuel costs per period.

Period	Gas (US\$/MBTU)	Diesel (US\$/MBTU)	Coal (US\$/MBTU)
2020	12.64	18.05	4.12
2022	13.04	21.42	4.19
2024	13.45	23.03	4.26
2026	13.80	24.52	4.32
2028	14.17	26.10	4.39
2030	14.39	27.12	4.43
2032	14.86	29.31	4.51
2034	15.35	31.50	4.56
2036	15.78	33.24	4.66
2038	16.22	34.50	4.73

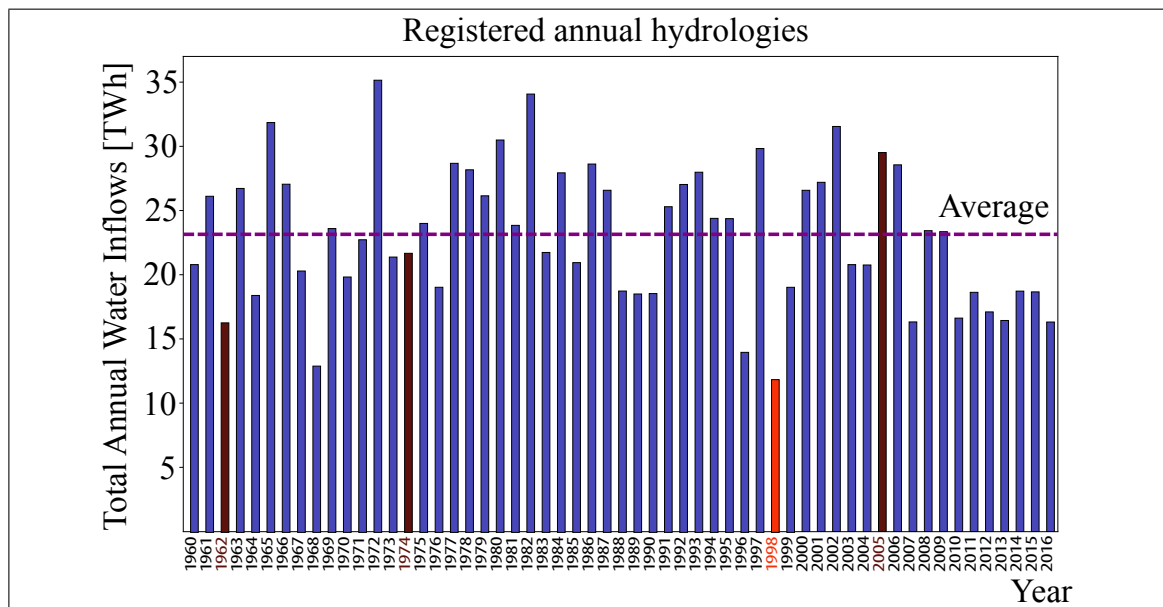


Figure A.1. Total water inflows per registered annual hydrology in units of electric energy, with representative and extreme hydrologies highlighted.

Table A.4. Transmission lines.

Transmission Line	Length (km)	η^L	Existing Capacity (MW)	$\overline{B^L}$ (MW)
Alto_Jahuel-Ancoa	335	0.985	2800	5000
Alto_Jahuel-Itahue	185	0.980	800	2000
Alto_Jahuel-Rapel	119	0.980	386	2000
Ancoa-Charrua	190	0.990	2600	4000
Cardones-Maitencillo	265	0.990	3400	4500
Charrua-Hualpen	72	0.980	1130	2000
Charrua-Temuco	205	0.980	1000	2000
Encuentro-Laberinto	133	0.990	800	2000
Encuentro-Mejillones	153	0.990	800	2000
DdAlmagro-Cardones	148	0.980	400	3000
Itahue-Ancoa	160	0.980	300	1000
Lagunas-Encuentro	173	0.990	800	2000
Los_Vilos-Nogales	97	0.985	446	2000
Maitencillo-PdAzucar	207	0.985	3400	5000
Mejillones-Cardones	600	0.970	3000	5000
Mejillones-Laberinto	205	0.990	800	2000
Nogales-Polpaico	84	0.990	3000	4000
Nogales-Quillota	27	0.990	446	1000
PdAzucar-Los_Vilos	228	0.985	900	2000
PdAzucar-Polpaico	405	0.970	3400	2000
Polpaico-Alto_Jahuel	72	0.990	4000	6000
Quillota-Polpaico	50	0.990	2000	3000
Temuco-Pto_Montt	370	0.980	600	2000

Table A.5. Transmission line parameters.

Overnight Cost (US\$/MW/km)	Project Lifetime (Years)	Fixed O&M Costs (US\$/MW)
1000	30	30